Chemistry of Copper Overlayers on Zinc Oxide Single-Crystal Surfaces: Model Active Sites for Cu/ZnO Methanol Synthesis Catalysts

Stephen V. Didziulis, Kristine D. Butcher, Susan L. Cohen, and Edward I. Solomon*

Contribution from the Department of Chemistry, Stanford University, Stanford, California 94305. *Received August 15, 1988*

Abstract: Copper has been evaporated onto chemically different single-crystal surfaces of zinc oxide in ultrahigh vacuum to model Cu/ZnO methanol synthesis catalysts. The formation of the copper overlayers from less than 0.1 monolayer (ML) to several ML on the (0001), (000$\bar{1}$), and (10$\bar{1}$0) surface planes is followed with core-level X-ray photoelectron spectroscopy, valence band photoelectron spectroscopy with both resonance discharge sources and synchrotron radiation, and low-energy electron diffraction. At room temperature, the first monolayer grows in a two-dimensional fashion, with low coverage copper existing as isolated atoms/small islands on all surfaces. Surface perturbations show submonolayer copper supported on the Zn^{2+}-terminated (0001) surface to be most prone to high-temperature clustering and reaction with molecular oxygen. Copper on the oxide-terminated (000$\bar{1}$) surface is much less reactive, while copper on the (10$\bar{1}$0) dimer surface shows intermediate reactivity. Low-temperature carbon monoxide (CO) chemisorption experiments indicate that highly dispersed copper on the (0001) and (10$\bar{1}$0) surfaces chemisorb CO with approximately the same affinity as copper metal (ΔH_{ads} = 15–16 kcal/mol), while chemisorption on Cu/(000$\bar{1}$) was much weaker (ΔH_{ads} < 12 kcal/mol). High-affinity (ΔH_{ads} = 21 kcal/mol) CO chemisorption, often associated with the catalytic active site, is shown to occur at a coordinatively unsaturated tetrahedral Cu^+ site created on the (0001) surface upon annealing in oxygen. Chemisorption to the Cu^+ site perturbs the CO electronic structure to a much greater extent than chemisorption to either Cu^0 or Zn^{2+}, with valence band PES indicating both strong σ and π interactions. The implications of these results with respect to CO activation and the catalytic activity of the Cu/ZnO system are discussed.

The reactivity of metal oxides in heterogeneous catalytic reactions is often quite different from that of metals. As an example, carbon monoxide is hydrogenated to methane over nickel catalysts, but with zinc oxide catalysts, the reaction goes selectively to methanol, where the C–O bond has been sustained:

$$CO + 2H_2 \Leftrightarrow CH_3OH \quad (1)$$

This reactivity is related to the nature of the inorganic complexes formed on the metal oxide surface, where the reactive molecules are bound to metal cations rather than electron-rich metal surfaces. As demonstrated in past experiments,[1-5] the carbon monoxide molecule binds carbon end down to coordinatively unsaturated zinc ions on the three different zinc oxide surfaces shown in Figure 1: the two hexagonal polar surfaces, (0001) and (000$\bar{1}$) having coordinatively unsaturated zinc or oxide ions respectively, and the nonpolar (10$\bar{1}$0) surface having equal numbers of zinc and oxide ions in dimer sites. The principle bonding interaction between the zinc ion and the CO molecule is the stabilization of the CO 5σ orbital via a σ-donor interaction with the empty Zn 4s and 4p levels. The Zn 3d levels are at very deep binding energy relative to the empty CO 2π* level, precluding any significant π-backbonding. This is consistent with the *increase* in the C–O stretching frequency of the ZnO bound molecule relative to the gas phase observed in high-resolution electron energy loss spectroscopic studies. A normal-coordinate analysis of this complex that included the Zn–C stretch produced an increase in the C–O force constant of the chemisorbed molecule, implying no backbonding into the 2π* antibonding level, which normally decreases the CO bond strength.[6] The net electronic effect in CO chemisorption on ZnO is the donation of electron density from the slightly antibonding 5σ level to the Zn^{2+} ion leading to a strengthened C–O bond while polarizing the CO molecule with a partial positive charge on the carbon atom and perhaps activating it for attack by adsorbed hydride ions.

Although highly selective, the methanol synthesis reaction with ZnO catalysts must be run under severe conditions (573–673 K under 150–200 atm of reaction gases) to achieve significant activity. The synthesis with the copper-promoted (Cu/ZnO) catalysts is also highly selective; however, the catalysts are active at 473–523 K and used industrially at pressures of 50–100 atm[7] as the activation barrier for methanol synthesis is only 18 kcal/mol with Cu/ZnO as compared to ~30 kcal/mol on ZnO.[8] Metallic copper is reported to show no measurable activity.[8,9] Additionally, a significant amount of CO chemisorbs to the Cu-promoted catalyst more strongly than to either Cu or ZnO, indicating that the Cu/ZnO combination contains a detectable number of surface sites unique to the mixture that could be important in the catalytic process. It is also important to note that methanol synthesis with the Cu/ZnO catalysts is much more efficient with CO_2 added in the reaction mixture. Both ZnO and Cu/ZnO catalysts normally contain an additional component, Al_2O_3 or Cr_2O_3, as an intracrystalline promoter functioning as a structural support to keep the catalyst dispersed.

A number of research groups have studied Cu/ZnO catalysts in a variety of forms (precursor, calcined, and reduced; binary and ternary) with a variety of physical methods in an attempt to determine the active site. Klier and co-workers[10-16] principally studied binary catalyst powders of varying Cu content (0–100%) with scanning transmission electron microscopy (STEM) and X-ray diffraction (XRD) to determine catalyst morphology, as

(1) Gay, R. R.; Nodine, M. H.; Henrich, V. E.; Zeiger, H. J.; Solomon, E. I. *J. Am. Chem. Soc.* **1980**, *102*, 6752.
(2) Sayers, M. J.; McClellan, M. R.; Gay, R. R.; Solomon, E. I.; McFeely, F. R. *Chem. Phys. Lett.* **1980**, *75*, 575.
(3) D'Amico, K. L.; McClellan, M. R.; Sayers, M. J.; Gay, R. R.; McFeely, F. R.; Solomon, E. I. *J. Vac. Sci. Technol.* **1980** *17*, 1080.
(4) McClellan, M. R.; Trenary, M.; Shinn, N. D.; Sayers, M. J.; D'Amico, K. L.; Solomon, E. I.; McFeely, F. R. *J. Chem. Phys.* **1981**, *74*, 4726.
(5) D'Amico, K. L.; Trenary, M.; Shinn, N. D.; Solomon, E. I.; McFeely, F. R. *J. Am. Chem. Soc.* **1982**, *104*, 5102.
(6) D'Amico, K. L.; McFeely, F. R.; Solomon, E. I. *J. Am. Chem. Soc.* **1983**, *105*, 6380.
(7) Natta, G. *Catalysis* **1955**, *3*, 349.
(8) Satterfield, C. N. *Heterogeneous Catalysis in Practice*; McGraw Hill: New York, 1980.
(9) Emmett, P. H. In *Catalysis Then and Now*; Emmett, P. H., Sabbatier, P., Reid, E. E., Eds.; Franklin Publishing: Englewood, NJ, 1965.
(10) Klier, K. *Adv. Catal.* **1982**, *31*, 243.
(11) Herman, R. G.; Klier, K.; Simmons, G. W.; Finn, B. P.; Bulko, J. B.; Kobylinski, T. B. *J. Catal.* **1979**, *56*, 407.
(12) Mehta, S.; Simmons, G. W.; Klier, K.; Herman, R. G. *J. Catal.* **1979**, *57*, 339.
(13) Bulko, J. B.; Herman, R. G.; Klier, K.; Simmons, G. W. *J. Phys. Chem.* **1979**, *83*, 3118.
(14) Klier, K.; Chatikavanij, V.; Herman, R. G.; Simmons, G. W. *J. Catal.* **1982**, *74*, 343.
(15) Dominquez, J. M.; Simmons, G. W.; Klier, K. *J. Mol. Catal.* **1983**, *20*, 369.
(16) Klier, K. *Appl. Surf. Sci.* **1984**, *19*, 267.

0002-7863/89/1511-7110$01.50/0

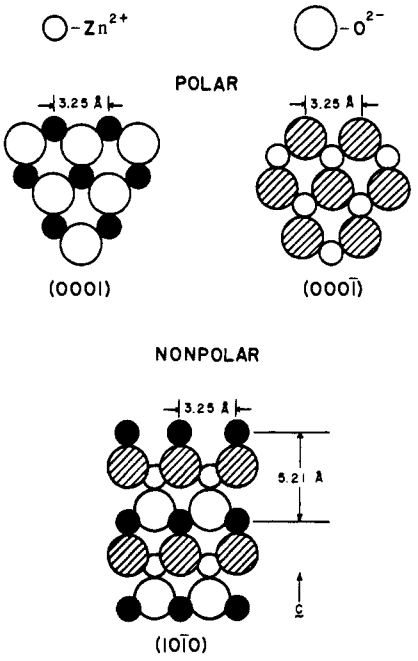

Figure 1. Space-filling representations of the ideal low-index ZnO surfaces as viewed from above with the shaded spheres representing surface ions.

well as diffuse reflectance spectroscopy and chemisorption of reaction gases in combination with catalyst activity studies. Klier determined that the ZnO component of the catalyst has two distinct morphologies which depend on the copper concentration. In low-concentration powders up to 30/70, the predominant ZnO surface exposed is the nonpolar (10$\bar{1}$0), while catalysts with higher Cu loadings (40/60 to 67/33) have primarily polar ZnO surfaces exposed. Upon reduction, approximately half of the copper in the most active 30/70 catalysts is contained in large, 20–200 Å, copper metal particles. The remaining copper is not detectable by STEM or XRD, implying that it exists in highly dispersed forms, either as very small Cu crystallites or doped into the ZnO lattice. Diffuse reflectance optical experiments reveal a feature at 17 500 cm^{-1} (2.17 eV) which is not present in either pure ZnO or Cu and is most intense in the most active catalyst. This transition energy is quite close to the bandgap transition of Cu_2O (2.2 eV)[17] and was assigned as arising from a Cu^+ 3d → ZnO conduction band (4s) transition with the cuprous ion substituted for Zn^{2+} in the crystalline lattice[10] or as Cu_2O.[18] A recent theoretical study by Rodriquez and Campbell, however, claims that copper substituted into the ZnO lattice should have a formal oxidation state of +2.[19] Alternatively, several research groups[20-22] contend that the active phase is copper metal with ZnO acting as either simply a structural support, the active site for hydrogen cleavage, or a reactant with poisons (primarily H_2S) in the gas mixture necessary to maintain catalyst activity.

The role of CO_2 in the catalytic process is still controversial, with possibilities including its direct conversion to CH_3OH, or the maintenance of catalyst activity through the oxidation of the surface active sites. Experimental work has suggested that the role of CO_2 in the feed gas mixture is to maintain the active site in an oxidized state. A $Cu/ZnO/Al_2O_3$ catalyst treated with CO_2 and H_2 developed an absorption feature similar to that seen in Klier's work which was assigned as arising from a Cu_2O phase.[18] In another recent study,[23] a 60/30/10 catalyst was treated with reaction gas mixtures containing $CO/CO_2/H_2/N_2$ in several different proportions at temperatures of 523–553 K. The number of oxygen-covered Cu sites following the treatment was shown to be proportional to the amount of CO_2 present in the feed gas.

Limited electron spectroscopic work (XPS and X-ray-induced Auger) has been done to determine the oxidation states and chemical environment of the surface copper phases in the catalyst, with contradictory results. These methods have several difficulties as there is normally no chemical shift of Cu^+ XPS core levels relative to Cu^0 and the LMM Auger features of Cu (which do show large energy shifts with oxidation state) strongly overlap Zn Auger features. Two groups have performed these experiments and found that the reduction process definitely eliminates all cupric ions, but while one group claims to see contribution from Cu^+ ions,[24] the other states that only Cu^0 is present.[25] A third study used the X-ray-induced Auger features of a Cu/Cr_2O_3-active methanol synthesis catalyst to unambiguously show the presence of cuprous ions as there is no interference from support features in the Cu LMM Auger region.[26] This catalyst is obviously different from the Cu/ZnO powders, but its activity was directly related to the intensity of the Cu^+ Auger signal.

Cu K-edge X-ray absorption spectroscopy (XAS) and extended X-ray absorption fine structure (EXAFS) experiments have also generated contradictory results. In one study, the Cu K-edge and EXAFS of reduced 24–30% Cu catalysts were interpreted as containing only Cu metal, but in highly dispersed forms.[27,28] A second study on a 30% Cu-reduced catalyst reports the existence of a Cu–O phase at room temperature, which appears to reversibly change to small Cu clusters (proposed as the active site) under H_2 at reaction temperatures.[29] The catalyst undergoes an irreversible transition to large Cu particles when heated to 400 °C, a process known to deactivate the catalyst. A third study of 30% reduced catalysts reports the existence of three phases, Cu metal, a Cu_2O-like phase, and Cu^+ ions apparently substituted in the ZnO lattice, but with unreasonable bond distances.[30]

To complement the work presented here and to define the types of copper present in the dispersed phase, our group has used Cu K-edge XAS and EXAFS to study several low-concentration (1–10% Cu) catalysts in the calcined form and reduced with both H_2/N_2, $CO/H_2/N_2$, and $CO/CO_2/H_2/N_2$ (reaction mixtures).[31,32] This work is discussed in the preceding paper. In the calcined (inactive, oxidized) form, there is evidence for some Cu^{2+} ions dissolved in the ZnO lattice. The two reduction mixtures produce different catalyst morphologies, with the catalysts reduced in H_2 having a higher percentage of large copper metal particles, while using the reaction mixture produces more highly dispersed Cu particles and an increased Cu–O phase with both Cu_2O and Cu^+ substituted into the ZnO lattice present. In addition, the amount of Cu^+ substituted into the ZnO lattice is greatest following reduction with CO_2-containing mixtures. Both small copper clusters and Cu(I) sites, therefore, are present in the dispersed phase on ZnO.

As mentioned above, the chemisorption behavior of the catalyst is different from the individual components. Klier[10,11] showed at least two forms of CO chemisorption to occur on reduced Cu/ZnO catalysts, one reversible at room temperature and a second

(17) Kleinman, L.; Mednick, K. *Phys. Rev. B* **1980**, *21*, 1549.
(18) Chinchen, G. C.; Waugh, K. C. *J. Catal.* **1986**, *97*, 280.
(19) Rodriquez, J. A.; Campbell, C. T. *J. Phys. Chem.* **1987**, *91*, 6648.
(20) Fleisch, T. H.; Mieville, R. L. *J. Catal.* **1986**, *97*, 284, and references therein.
(21) Friedrich, J. B.; Wainwright, M. S.; Young, D. J. *J. Catal.* **1983**, *80*, 1.
(22) Marsden, W. L.; Wainwright, M. S.; Friedrich, J. B. *Ind. Eng. Chem. Prod. Dev.* **1980**, *19*, 551.
(23) Baussart, H.; Delobel, R.; Le Bras, M.; Le Maguer, D.; Leroy, J. M. *Appl. Catal.* **1985**, *14*, 381.
(24) Okamoto, Y.; Fukino, K.; Imanaka, T.; Teranishi, S. *J. Phys. Chem.* **1983**, *87*, 3747.
(25) Fleisch, T. H.; Mieville, R. L. *J. Catal.* **1984**, *90*, 165.
(26) Apai, G.; Monnier, J. R.; Hanrahan, M. J. *Appl. Surf. Sci.* **1984**, *19*, 307.
(27) Vlaic, G.; Bart, J. C. J.; Cavigiolo, W.; Mobilio, S. *Chem. Phys. Lett.* **1980**, *76*, 453.
(28) Vlaic, G.; Bart, J. C. J.; Cavigiolo, W.; Pianzola, B.; Mobilio, S. *J. Catal.* **1985**, *96*, 314.
(29) Tohji, K.; Udagawa, Y.; Mizushima, T.; Ueno, A. *J. Phys. Chem.* **1985**, *89*, 5671.
(30) Sankar, G.; Vasudevan, S.; Rao, C. N. R. *J. Chem. Phys.* **1986**, *85*, 2291.
(31) Kao, L. S.; Solomon, E. I.; Hodgson, K. O. *J. Phys. (Paris)* **1986**, *47*, C8.
(32) Kao, L. S. Ph.D. Thesis, Stanford University, 1988.

"irreversible", that is, did not pump off in 10^{-6}-Torr vacuum in 10 min. The amount of irreversible CO adsorbed was greatest on the most active catalysts.[10] The CO chemisorption behavior of an apparently overreduced catalyst by using temperature-programmed desorption showed three forms of chemisorbed CO.[33] A 12 kcal/mol species is definitely chemisorption on Zn^{2+} sites,[1] while the other two forms were attributed to adsorption on Cu sites, one having E_d = 14–16 kcal/mol and a second with E_d = 18 kcal/mol, assigned as a Cu^+ chemisorption site. The 14–16 kcal/mol values are consistent with the surface science literature for CO adsorption on Cu metal,[34-37] while CO chemisorption on Cu^+ in a zeolite framework was irreversible under the criteria stated above.[38]

With the many contradictory results of the physical characterizations outlined above, much confusion still exists over the nature of the catalytic active site in the Cu/ZnO system. The most systematic of the studies indicates that copper must exist in a variety of forms in the catalyst. Since both components are needed for the enhanced reactivity, a Cu site in intimate contact with a ZnO surface, either the highly dispersed Cu metal or a surface Cu^+ site, is likely involved in the catalysis. While there has been limited experimental work on thin Cu films on ZnO single crystal[39,40] and polycrystalline surfaces,[41] no work aimed at understanding the effects of the supporting ZnO surface on the properties of the highly dispersed Cu phase has been conducted. The work presented here is aimed at simplifying the complex nature of the Cu/ZnO system through the preparation and characterization of specific copper sites on the catalytically important, low-index surfaces of ZnO in ultrahigh vacuum. First, the interaction and reactivity of copper deposited on chemically different ZnO surfaces is investigated to determine if specific ZnO surfaces provide sites for Cu species having unique reactivity. Second, different surface sites corresponding to the various proposed active sites composed of well-dispersed Cu, oxidized Cu, and large Cu particles are prepared and characterized. Finally, the CO chemisorption behavior of these sites is investigated to define the specific surface site associated with high affinity CO chemisorption.

Well-regulated amounts of Cu are evaporated onto the ZnO surfaces in Figure 1 in ultrahigh vacuum (UHV) to produce the model surfaces, and surface-sensitive electron spectroscopies are used in combination with a variety of perturbations to study the electronic structure and reactivity of the Cu/ZnO combinations. As the dispersed Cu phases seem to be of the most interest for methanol synthesis, perturbations of low coverage (0.3 ML) overlayers are pursued. The perturbations include heating to temperatures at and above the methanol synthesis reaction temperatures and oxygen treatments to study the oxidation properties of the Cu sites. These treatments also produce a variety of copper sites in different oxidation states that allow the study of CO adsorption to definitively determine the site of the high-affinity CO chemisorption.

The principle method used to study the Cu/ZnO surfaces is photoelectron spectroscopy (PES) with vacuum-ultraviolet, X-ray, and synchrotron radiation. X-ray photoelectron spectroscopy (XPS) of both overlayer and substrate core levels is used to monitor the amount of Cu present and to study the overlayer growth mode by following changes in the peak intensities, binding energies, and widths as a function of copper coverage. PES with both vacuum-UV (He I and He II) and synchrotron radiation is employed to determine the valence band electronic structure of the Cu/ZnO systems. Synchrotron radiation is of particular utility in this study as it allows the distinction between overlayer and substrate PES features through changes in photoionization cross sections and an enhancement of the surface sensitivity of the spectroscopy. In addition, resonance PES at the Cu 3p absorption edge enhances the intensity of particular copper valence levels that provide insight into the oxidation state of the submonolayer surface Cu sites.

Experimental Section

Single-crystal $(10\bar{1}0)$, (0001), and $(000\bar{1})$ surfaces of ZnO were prepared by aligning the crystal to within 1° of the desired plane by Laue back-diffraction and then cutting a slice approximately 1 mm thick with a wire saw. The crystals were polished by hand with alumina grit down to 0.5 μm until no pits were evident with optical microscopy. The surfaces were then chemically polished with dilute (5%) HCl. The acid etch also allows the $(000\bar{1})$ and (0001) surfaces to be distinguished[42,43] as the oxide surface is visibly etched more quickly and extensively than the Zn surface.[44] The samples were mounted on molybdenum sample holders after being wrapped in platinum foil to improve thermal contact. The Pt foil was spot welded to or held by screws on the molybdenum sample holders.

Cleaning in UHV was performed by Ar^+ ion sputtering at successively lower accelerating potentials of 1 kV, 500 V, and 250 V [to minimize sample damage] with beam currents of 1–5 $\mu A/cm^2$ while heating to 723 K. Sample cleanliness was monitored with Auger using a 2-keV, 0.5-μA electron beam and lock-in detection with 5-V peak-to-peak modulation. Sputter cycles were repeated until no contaminants (<1% C, S, Cl) were observed, and the sample was then annealed two additional times to 723 K. Surface order was checked with low-energy electron diffraction (LEED) with (1 × 1) patterns obtained after the above treatments. The LEED patterns of the hexagonal polar surfaces usually show some spot splitting or streaking from double-layer steps exposing $(10\bar{1}0)$ sites which act to relieve the surface charge associated with an ideal polar plane.[45]

Copper was evaporated onto the single-crystal ZnO surfaces with a resistively heated high-purity Cu bead on a tungsten filament. Approximately 3 A of current was needed to achieve Cu evaporation (which occurs near 1200 K) at the desired rate of between 1 and 2 Å/min. The evaporation rate was monitored with a quartz crystal oscillator thickness monitor [R. D. Mathis Co. Model TM-100] using 5-MHz gold-coated crystals. The density was programmed into the controller at one-tenth the real value of Cu, giving the monitor 0.1-Å thickness resolution. Once a steady evaporation rate was achieved (±0.1 Å/min, for several minutes), the evaporator shutter was closed and the sample moved into position replacing the quartz monitor crystal. The shutter was then opened for the time needed to achieve the desired coverage, usually in increments of "0.2" to "0.4" Å, readings which represent an average layer thickness and correspond to a certain fraction of a monolayer (vide infra). The ZnO substrates were maintained at room temperature for all evaporations. The pressure remained less than 5×10^{-10} Torr during evaporations, only slightly higher than the operating pressure of 2×10^{-10} Torr.

Photoelectron spectroscopic probes included the core level XPS of both ZnO substrate and Cu overlayer and variable photon energy valence band PES of the Cu/ZnO surfaces. The XPS work was conducted with Mg Kα radiation (1253.6 eV) in a Vacuum Generators ESCALAB Mk II instrument with a hemispherical analyzer and single-channel detection described in detail elsewhere.[46] The X-ray anode was generally run at 100 W, but 150 W was used when studying very low coverages (<0.2 Å). An analyzer pass energy of 20 eV was used to ensure sufficient resolution to accurately determine binding energy positions and shapes of the Cu $2p_{3/2}$, Zn $2p_{3/2}$, and O 1s peaks.

The development of copper valence levels as a function of overlayer coverage and perturbation of the Cu/ZnO surfaces was studied in the ESCALAB using He I (21.2 eV) and He II (40.8 eV) resonance lines. He I spectra with a −9 V sample bias were used to determine the work function of the surfaces from the low kinetic energy cutoff of the secondary electron tail. Synchrotron radiation in the photon-energy range 30–120 eV from the Grasshopper monochromator on SPEAR beam line III-1 at the Stanford Synchrotron Radiation Laboratory (SSRL) was also used to obtain valence band data. A Perkin-Elmer vacuum chamber with a double-pass CMA described elsewhere[46] was used with the evaporation equipment detailed above. The pass energy for the CMA was

(33) Roberts, D. L.; Griffin, G. L. *Appl. Surf. Sci.* **1984**, *19*, 298.
(34) Tracy, J. C. *J. Chem. Phys.* **1972**, *56*, 2748.
(35) Pritchard, J. *J. Vac. Sci. Technol.* **1972**, *9*, 895.
(36) Wachs, L. E.; Madix, R. J. *J. Catal.* **1978**, *53*, 208.
(37) Alexander, C. S.; Pritchard, J. *J. Chem. Soc., Faraday Trans 1* **1972**, *68*, 202.
(38) Huang, Y. *J. Catal.* **1973**, *30*, 187.
(39) Campbell, C. T.; Daube, K. A.; White, J. M. *Surf. Sci.* **1987**, *182*, 458.
(40) Mokwa, W.; Kohl, D.; Heiland, G. *Fresenius Z. Anal. Chem.* **1983**, *314*, 315.
(41) Chan, L.; Griffen, G. L. *Surf. Sci.* **1986**, *173*, 160.
(42) Klein, A. *Z. Phys.* **1965**, *188*, 352.
(43) Heiland, G.; Kunstman, P. *Surf. Sci.* **1969**, *13*, 72.
(44) The surfaces were further characterized in UHV by their measured work functions and UPS spectra to ensure the correctness of this assignment.
(45) Kohl, D.; Henzler, M.; Heiland, G. *Surf. Sci.* **1974**, *41*, 403.
(46) Didziulis, S. V.; Cohen, S. L.; Gewirth, A. A.; Solomon, E. I. *J. Am. Chem. Soc.* **1988**, *110*, 250.

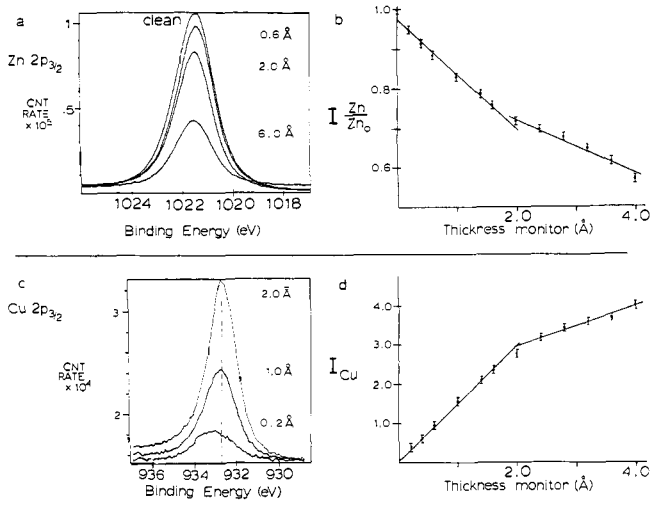

Figure 2. XPS core levels and their integrated intensities as a function of Cu coverage on ZnO (000$\bar{1}$): (a) Zn $2p_{3/2}$ peak, (b) Zn $2p_{3/2}$ intensity, (c) Cu $2p_{3/2}$ peak, (d) Cu $2p_{3/2}$ intensity.

set at 25 eV, and the AES analyzer slits were used. The radiation impinged on the sample at nearly grazing incidence, with the polarization vector aligned parallel to the surface normal and the central axis of the CMA. As the acceptance angle of this detector is 42.3 ± 3° off normal, the effects of polarization on the d and oxide band substrate photoemission should be fairly limited. This is confirmed by the similar spectral intensities obtained for polycrystalline and (111) single-crystal samples of CuCl. The monochromator slits were adjusted to maintain a constant photon energy resolution of 200 meV, and the appropriate transmission filters were used to limit higher order diffracted radiation.[47,48] All spectra taken at the synchrotron were normalized to the incident photon flux with a flux monitor consisting of a nickel or stainless steel mesh in the path of the monochromatic radiation and total yield channeltron detector. The number of photoelectrons detected from the mesh is proportional to the incident photon flux, and this signal was collected along with the signal-averaged data.[49]

Resonance PES data at the Cu 3p absorption edge near photon energies of 75–80 eV were obtained under the same conditions as listed above. Constant initial state (CIS) intensity profiles of the resonantly enhanced features were obtained by scanning the photon energy and analyzed kinetic energy such that the intensity of a peak at constant binding energy is obtained. For all CIS spectra, the beam line slits were adjusted such that the photon energy resolution was better than 200 meV at all photon energies in the scan. The pass energy was increased to 50 eV to increase the signal to noise for study of the very weak satellite peaks.

Submonolayer (0.6 Å) copper overlayers on the ZnO surfaces were subjected to both heating in vacuum and oxygen exposures. The heating was performed with resistively heated filaments in the sample holders, and the temperature was monitored by a chromel–alumel thermocouple in direct contact with the sample holder. Oxygen exposures at room and elevated temperatures were performed by backfilling the vacuum chamber with research-purity O_2 (Matheson, 99.99%) through a Varian leak valve with the pressure monitored by a nude ionization gauge. The prepared Cu model sites were exposed to CO (Matheson research purity, 99.99%) in the ESCALAB at low temperatures (120–273 K) with the chemisorption behavior monitored by He II UPS. The diffusion pump gate valve was left open during data collection in 10^{-6}-Torr ambients, and the valve was throttled at higher ambient pressures. It was necessary to do so as the pressure increase arising from the discharge lamp was significant with the pump valved off.

Results and Analysis

(A) Cu Overlayer: Growth and Electronic Structure. (1) Core Level XPS and LEED. The changes in the Zn $2p_{3/2}$ and Cu $2p_{3/2}$ XPS core levels with increasing amounts of copper evaporated onto the ZnO (000$\bar{1}$) surface are shown in Figure 2. As expected for overlayer formation, the substrate Zn $2p_{3/2}$ peak intensity

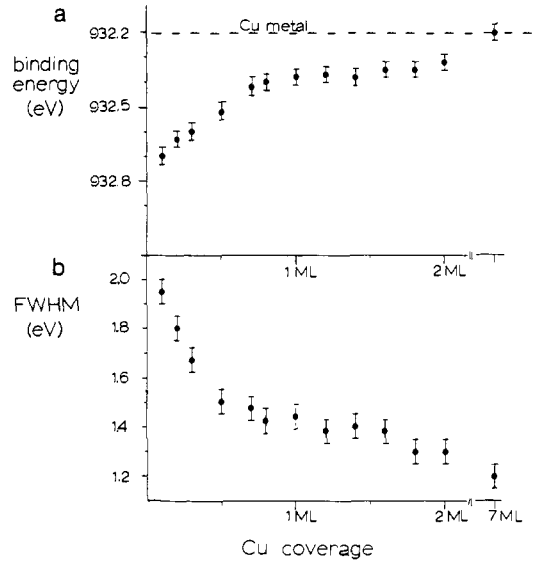

Figure 3. Cu $2p_{3/2}$ peak binding energy (a) and full width at half-maximum (b) as a function of coverage on ZnO (000$\bar{1}$).

(Figure 2a) is attenuated with increasing copper deposition due to the finite photoelectron escape depth. A plot of the integrated Zn $2p_{3/2}$ intensity relative to the clean substrate intensity (I_θ/I_0) versus the total Cu exposure is also given in Figure 2b. This plot gives the average of three different experiments on (000$\bar{1}$) and shows an essentially linear intensity decrease up to 2.0 Å of Cu. Near the 2.0-Å point, the slope of the intensity decrease changes before continuing to decline at higher coverages. The linear intensity decrease is characteristic of two dimensional (laminar) overlayer growth[50] as described for the first monolayer by the equation

$$I_\theta/I_0 = 1 - \theta(1 + e^{-d/\lambda}) \qquad (2)$$

where I_0 is the substrate peak intensity at zero coverage, θ is the fractional overlayer coverage [expressed in monolayers (ML)], and the exponential term describes the attenuation of the substrate photoelectron peak intensity by the metal overlayer of thickness d and a finite electron escape depth (λ). The slope change at 2.0 Å indicates the point at which a monolayer has been completed, and coverages will henceforth be given in units of monolayers where 1 ML = 2.0 Å. The values of $\theta = 1$ and $d = 2.0$ Å at the 1-ML cutoff allow the determination of the electron escape depth (λ) as 6.0 ± 1.0 Å for electrons having kinetic energies of 230 eV through a copper layer.[51] This value is in reasonable agreement with both experimental and theoretical evaluations[52] of the electron scattering length in copper, and hence fits nicely on the "universal curve" of electron escape depths. These results also support the laminar growth mechanism for at least the first overlayer as extensive three-dimensional clustering requires an extremely short scattering length to achieve the same intensity attenuation. The O 1s XPS peak of the ZnO substrate was obtained as a function of coverage. Average intensity ratios at 1 and 2 ML of 0.85 and 0.72 give an escape depth of ~12 Å for the electrons having kinetic energies of 723 eV, a reasonably larger value for these higher kinetic energy electrons.

Laminar Cu overlayer growth on (000$\bar{1}$) is also indicated by the intensity changes of the Cu $2p_{3/2}$ peak with coverage shown and plotted in Figure 2c,d. The Cu peak intensity increases linearly up to 2.0 Å, before showing a sharp change in slope as seen with the substrate peak intensity. In addition, the Cu $2p_{3/2}$

(47) Stohr, J. *Instruction Manual for the New Grasshopper Monochromator*; Stanford Synchrotron Radiation Laboratory: Stanford CA, 1980.
(48) Pate, B. B. Ph.D. Thesis, Stanford University, 1984.
(49) Lindau, I.; Spicer, W. E. In *Synchrotron Radiation Research*; Winick, H., Doniach, S., Eds.: Plenum Press: New York, 1980.
(50) Phillips, L. V.; Salvati, L.; Carter, W. J.; Hercules, D. M. In *Quantitative Surface Analysis of Materials*; ASTM STP 643, McIntyre, N. S., Ed.; American Society for Testing and Materials, 1978; p 47.
(51) It should be noted that the distance between successive Cu (111) planes is 2.21 Å and if this value is used for d instead of 2.0 Å, then an escape depth of 6.2 Å is obtained.
(52) Tokutaka, H.; Nishimori, K.; Hayasi, H. *Surf. Sci.* **1985**, *149*, 349, and references therein.

peak shifts to lower binding energy relative to the substrate peak binding energies with increasing coverage as plotted in Figure 3a. The total Cu $2p_{3/2}$ binding energy shift from the value obtained at 0.1 ML until a metallic copper binding energy is achieved (at several monolayers) was generally 0.5–0.6 eV. This places the 0.1-ML Cu $2p_{3/2}$ level at 932.7–932.8 eV relative to the Fermi level with the binding energy of metallic Cu being 932.2 eV, our reference energy in this work.[53] At coverages up to 0.1 ML, very little shift in binding energy is observed. Similar binding energy shifts with increasing metal coverage have been observed for many other overlayer systems and are usually attributed to increased extra atomic final-state relaxation which occurs as more metal atoms come into contact providing increased electron density for final state screening.[54,55]

The Cu $2p_{3/2}$ peak at low coverage on ZnO is considerably broader than observed for Cu metal as shown in the spectra in Figure 2c and plotted in Figure 3b. The peak width is greater than 2 eV at the lowest coverages studied (<0.1 ML) and decreases with increasing Cu coverages, eventually attaining the same full width at half-maximum (fwhm) as an unoriented Cu sample, 1.20 eV. This broadening is also frequently observed for metal overlayers[55,56] and could have two sources: an intrinsically broad peak width or heterogeneity of surface sites displaying a spread of binding energies. The heterogeneity of sites can seemingly be excluded as the Cu-cluster sizes should be more homogeneous at very low coverage leading to narrow PES peaks. The peak width should go through a maximum at an intermediate coverage where copper clusters exist in a variety of sizes and then decrease as a homogeneous metal overlayer is formed. Theoretical work supports the existence of broad XPS peak widths for species having limited ability to screen the final state hole.[57] The broad Cu $2p_{3/2}$ peak at low coverage, therefore, is attributed to an intrinsic broadening from final-state relaxation effects.

LEED studies of the (000$\bar{1}$) surface after successive Cu evaporations show only the (1 × 1) hexagonal substrate pattern up to ~3-ML coverage. The ZnO pattern and the background become more diffuse with increasing Cu coverage, but the (1 × 1) pattern remains visible. At 6–8-Å coverage, a new and very weak, hexagonal (1 × 1) LEED pattern emerges with larger reciprocal lattice dimensions than the ZnO pattern. The new diffraction spots are rotationally aligned with the substrate diffraction spots. The difference in reciprocal lattice dimension correlates well to the smaller Cu–Cu bond distance of 2.56 Å on the Cu (111) surface relative to the 3.25-Å separation of the oxide ions on the ZnO (000$\bar{1}$) surface. These results suggest a random overlayer growth pattern in the submonolayer regime maintaining the ZnO lattice spacing as no ordered overlayer is observed. The copper eventually adopts its own fcc structure with increasing coverage and the aligned LEED patterns indicate epitaxial growth. Campbell et al.[39] report similar XPS intensity results and also observed the retention of the substrate (1 × 1) pattern and the formation of the Cu (111) LEED pattern at higher copper coverages on (000$\bar{1}$).

Copper evaporations on the (0001) and (10$\bar{1}$0) surfaces were also conducted, and several spectroscopic similarities to overlayer formation on (000$\bar{1}$) point to predominantly laminar overlayer growth at room temperature for at least the first monolayer on both (0001) and (10$\bar{1}$0). Specifically, Cu $2p_{3/2}$ final-state relaxation shifts on the order of 0.5 eV with increasing coverage from 0.1 ML, narrowing of the Cu $2p_{3/2}$ peak width with increasing coverage, and the similarity of the Zn $2p_{3/2}$ I_θ/I_0 ratio at particular coverages on the different surfaces support this

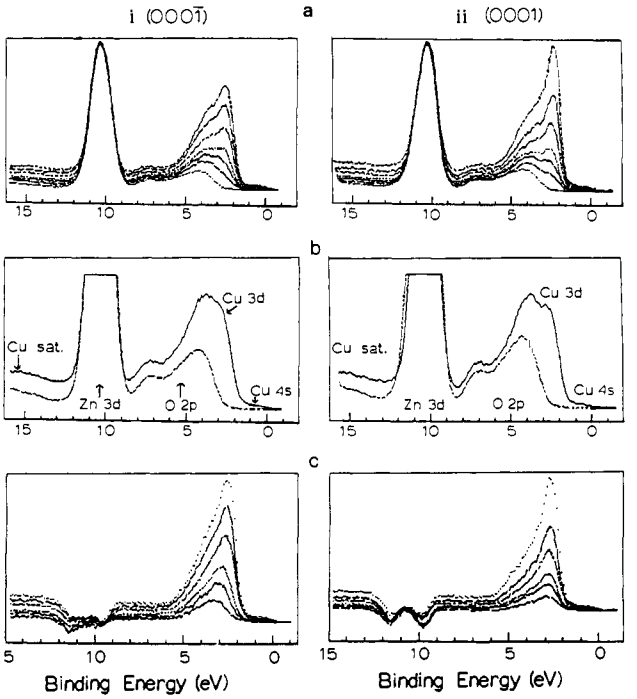

Figure 4. (a) Valence band PES data obtained with $h\nu$ = 120 eV for ZnO (i) (000$\bar{1}$) and (ii) (0001) with increasing copper coverage. From the bottom, the coverages are 0, 0.1, 0.2, 0.3, 0.5, 0.7, and 1.0 ML. The data have been normalized to the Zn 3d band intensity. (b) The 0.2-ML Cu data compared to clean ZnO for the two surfaces. (c) Valence difference spectra obtained by subtracting the clean spectra from the Cu overlayer spectra in (a).

growth mode. In addition, the (1 × 1) LEED patterns of the substrate are maintained throughout evaporation to 1 ML, with the substrate spots and background becoming more diffuse as with (000$\bar{1}$). At 15–20-Å coverage on (10$\bar{1}$0), a new set of diffraction spots are observed that appear to be rotationally aligned with the rectangular substrate pattern. The spots were too diffuse, however, to determine the precise symmetry of the new copper phase.

(2) Valence Band PES. The development of the copper valence band PES features with increasing coverage on (000$\bar{1}$) obtained at a photon energy of 120 eV is shown in Figure 4ai. In the clean ZnO spectrum at the bottom of the group of spectra, the peak near 10.5-eV binding energy results from ionization of Zn 3d levels while the group of peaks from 4–8 eV result from oxide 2p photoemission.[58] As expected from photoionization cross section effects, the intensities of the oxide PES peaks are significantly lower than the Zn 3d levels in the clean 120-eV spectra. The spectra show an increase in PES intensity at the top edge of the substrate O 2p valence band near binding energies of 3–4 eV with increasing Cu coverage; these changes are clearly seen in the difference spectra of Figure 4ci obtained by subtracting the clean ZnO spectrum from the copper overlayer spectra following normalization of the spectra to the Zn 3d peak intensity and shifting to account for band bending changes (vide infra). This intensity is due to Cu 3d states which have a very high PES cross section relative to the oxygen 2p levels at 120 eV. The Cu 3d levels shift to lower binding energy relative to the ZnO features with increasing coverage, with the total shift of 0.4–0.5 eV similar to the relaxation shift observed for the Cu core level. Significant PES intensity on the low binding energy side of the Cu 3d levels and in the bandgap of ZnO is observed at coverages as low as 0.2 ML as shown in Figure 4bi. This region develops a well-defined Fermi edge at higher coverages and is assigned as Cu 4s photoemission intensity as these states contribute most in this energy region in the band structure for copper metal. It is important to note that a well-defined Cu 4s peak is not observed at any cov-

(53) The actual measured binding energy at 0.1 ML is 933.2–933.3 eV, but band bending effects account for a large portion of the change to 932.2 eV with increasing coverage. The band-bending changes are subtracted from the binding-energy shifts given in Figure 3.

(54) Wertheim, G. K.; DiCenzo, S. B.; Youngquist, S. E. *Phys. Rev. Lett.* **1983**, *51*, 2310.

(55) Cheung, T. T. P. *Chem. Phys. Lett.* **1984**, *110*, 219.

(56) Mason, M. G.; Gerenser, L. J.; Lee, S. T. *Phys. Rev. Lett.* **1977**, *39*, 288.

(57) Fuggle, J. C.; Campagna, M.; Zolnierek, Z.; Lasser, R.; Platau, A. *Phys. Rev. Lett.* **1980**, *45*, 1597, and references therein.

(58) Didziulis, S. V.; Butcher, K. D.; Cohen, S. L.; Solomon, E. I. *Inorg. Chem.* **1988**, *27*, 2238.

Table I. Summary of Resonance PES Results for Several Copper Sites[a]

	satellite 3d splitting, eV	nonreson int, %	reson int, %	3p → 4s reson energy, eV	Coulomb repulsion (U), eV
0.3 ML/(000$\bar{1}$)	12.4	~2	10	75.5	8.9
0.3 ML/(0001)	12.5	~2	10	75.7	9.0
Cu metal[b]	11.4	<2	~10	75.6	8.2
10 ML/ZnO	11.7	1–2	10	75.8	8.1
Cu_2O[b]	12.0	~2	5	76.5	7.9
CuCl[c]	12.2	~1	11	76.9	8.5

[a] The satellite intensities are given relative to the main band intensity as a percentage. [b] From ref 62. [c] From ref 58.

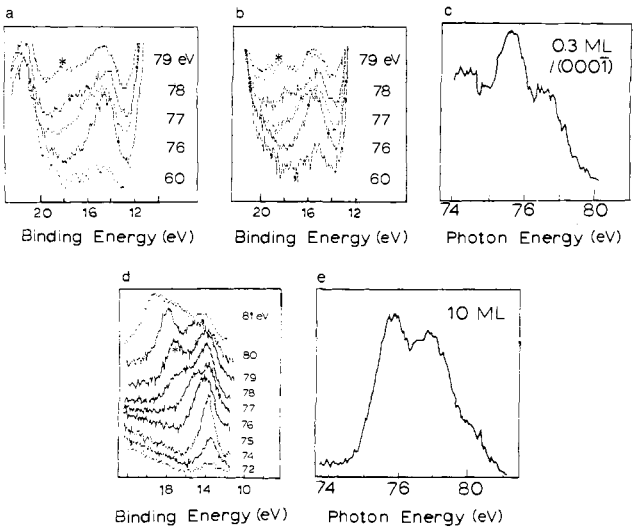

Figure 5. Resonance PES of the Cu multielectron satellite region for 0.3-ML coverage on (a) (000$\bar{1}$) and (b) (0001) are given with (c) the CIS satellite intensity profile for 0.3-ML/(000$\bar{1}$). Also included are the resonance data for the satellite (d) and the corresponding CIS intensity profile (e) of a 10 ML Cu/(0001) surface. The asterisk denotes the $M_{2,3}M_{4,5}M_{4,5}$ Auger peak.

erage. Although this peak would be quite weak (less than 10% of the d band intensity), it is still observed in the PES spectrum of Cu vapor at 3 eV above the d levels.[59] These facts indicate that the low-coverage supported copper is neither extensively oxidized (4s intensity is still present) nor atomic in nature and suggest that the 4s level is somewhat delocalized.

The valence band PES spectra at 120 eV for Cu overlayer formation on the (0001) surface in Figures 4aii, 4bii, and 4cii are similar to those observed on (000$\bar{1}$), with the Cu 3d levels developing at the top edge of the oxide valence band and 4s intensity observed in the ZnO bandgap region at low coverage as labeled in Figure 4. An interesting difference is that the low-coverage (≤0.3 ML) Cu 3d states on (0001) appear at 0.3–0.4 eV lower binding energies and do not show as large a shift to lower binding energy relative to the substrate energy levels with increasing coverage.[60]

He II data of the valence band of Cu on the (10$\bar{1}$0) surface indicate that the Cu 3d levels develop much the same as on (0001). The Cu 3d levels appear at the top edge of the oxide 2p band, not overlapping the oxide band as strongly as (000$\bar{1}$). In addition, the d levels show little shift to lower binding energy with increasing coverage, although these data are not as conclusive as the spectra obtained with synchrotron radiation.

As stated earlier, the Cu 2p core level binding energies and lack of shakeup satellites indicate that the highly dispersed copper is either Cu^0 or Cu^+. Resonant photoemission is a complex many-body process, but the photon energy at which resonance occurs and the nature of the resonance enhancement are quite sensitive to the chemical environment of the copper site and thus should allow the distinction between metallic copper and Cu^+. A very weak satellite peak between the Zn 3d and O 2s peaks near 15-eV binding energy in the valence band spectrum of the 0.3-ML Cu/(000$\bar{1}$) surface is enhanced in intensity by a factor of approximately 5–10 upon changing the photon energy from 60 to 76 eV as shown in Figure 5a. This peak is not present in the clean ZnO valence band spectrum. The satellite has ~10% of the copper d band intensity at 76 eV and the CIS resonance profile in Figure 5c[61] shows the maximum resonance enhancement occurs at 75.5 eV, which is the Cu 3p → 4s transition energy for copper metal.[62] Conversely, the resonance energies of the 0.3 ML/ZnO surfaces given in Table I are ~1 eV less than those of Cu_2O[62] and CuCl, where the energies of the antibonding 4s levels have been raised through ligand bonding interactions.[58] Since the copper 3p → 4s transition energies for the 0.3 ML/ZnO surfaces are the same as observed for copper metal, the relative energy splitting of the Cu 3p and 4s levels of the dispersed Cu is not significantly different than in Cu metal. These results show that the dispersed copper is Cu^0 and not Cu^+.

The enhancement of the satellite peak at the Cu 3p → 4s edge allows its assignment as the final state arising from Cu d ionization plus a Cu 3d → 4s shakeup transition. This assignment is demonstrated in Scheme I for Cu^0, where the excited state attained

Scheme I

d ionization: $3p^63d^{10}4s^1 \rightarrow 3p^63d^94s^1$

d ionization + shakeup: $3p^63d^{10}4s^1 \rightarrow 3p^63d^84s^2$

resonance: $3p^63d^{10}4s^1 \rightarrow 3p^53d^{10}4s^2 \rightarrow 3p^63d^84s^2$

$M_{2,3}M_{4,5}M_{4,5}$ Auger: $3p^63d^{10}4s^1 \rightarrow 3p^53d^{10}4s^1 \rightarrow 3p^63d^84s^1$

at the Cu 3p edge undergoes a highly allowed Super-Coster Kronig autoionization to a $3d^84s^2$ final state. A second peak (labeled with an asterisk in the 79-eV data) shifts to deeper binding energy with increasing photon energy in the spectra of Figure 5 and is a constant kinetic energy feature, leading to its assignment as an Auger electron peak. The Auger transition is obviously associated with the Cu 3p edge and is assigned as the Cu $M_{2,3}M_{4,5}M_{4,5}$ peak as indicated in Scheme I.

Important differences in the resonance PES behavior of the 0.3 ML Cu/(000$\bar{1}$) compared to copper metal exist. The differences include the larger Cu 3d satellite splitting for the submonolayer coverage (12.4 vs 11.7 eV, Table I) and the much weaker $M_{2,3}M_{4,5}M_{4,5}$ Auger peak accompanying the satellite peak (79-eV data in Figure 5a versus 5c). A weak Auger peak is seen both for oxidized Cu species[62] and in atomic Cu^0[63] relative to metallic Cu. As shown in eq 3, the d-band satellite splitting ($E_{sat.} - E_{3d}$)

$$E_{sat.} - E_{3d} = E_{3d \rightarrow 4s} + U \quad (3)$$

measured from the data is the sum of the Cu 3d → 4s ($E_{3d \rightarrow 4s}$) transition energy and the metal-centered electron–electron repulsion (U).[58] The value of U determined for the dispersed copper from the 0.3-ML data and eq 3 is 0.7–0.9 eV greater than for metallic copper, assuming that the copper 3d → 4s transition energy is the same for both species, which is reasonable as the 3p → 4s transition energies and the 3p–3d binding energy splittings

(59) Dyke, J. M.; Fayad, N. K.; Morris, A.; Trickle, I. R. *J. Phys. B: At. Mol. Phys.* **1979**, *12*, 2985.

(60) The 1-ML Cu/(0001) spectrum has more Cu 3d intensity than observed on (000$\bar{1}$), which indicates that a larger amount of Cu was evaporated onto this surface. The Cu 3d peak is also measurably narrower on (0001).

(61) The two-peak structure of the CIS data arises from the 2.2-eV spin-orbit splitting of the 3p hole.

(62) Thuler, M. R.; Benbow, R. L.; Hurych, Z. *Phys. Rev. B* **1982**, *26*, 669.

(63) Chandesris, D.; Guillot, C.; Chauvin, G.; Lecante, J.; Petroff, Y. *Phys. Rev. Lett.* **1981**, *47*, 1273.

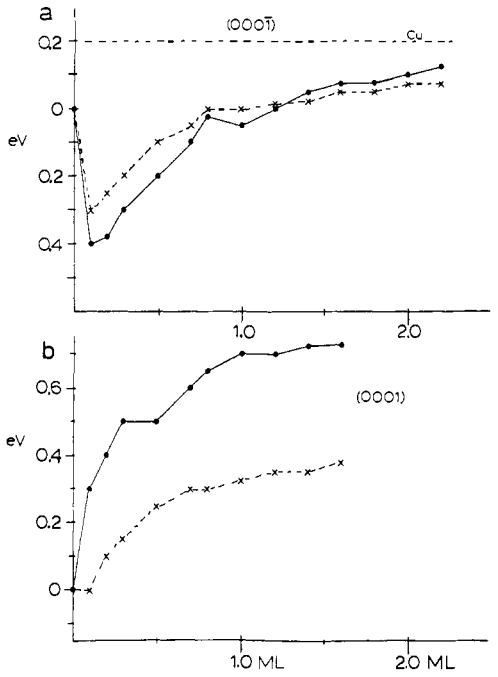

Figure 6. Band bending (×) and work function (●) changes with increasing Cu overlayer coverage for (a) (000$\bar{1}$) and (b) (0001).

are the same. This increase is consistent with the isolated nature of the copper sites as covalent interactions tend to lower repulsion through expansion of the d orbitals. The resonance PES of Cu vapor[63] is also quite different from either copper metal or what we observe for the 0.3-ML copper overlayer. The highly dispersed copper, therefore, displays unique resonance PES features showing that the copper is not purely metallic, atomic or oxidized. The resonance PES data for 0.3-ML Cu on (0001) is almost indistinguishable from the (000$\bar{1}$) surface as shown in Figure 5b and Table I.

The n-type semiconducting ZnO surfaces exhibit interesting band bending and work function changes upon deposition of copper. The extent of band bending was obtained from the Zn 3d binding energy in the valence band PES data and work function changes from the low kinetic energy cutoff of the secondary electron tail in the biased He I data. Evaporation of 0.1-ML Cu on (000$\bar{1}$) causes an abrupt downward band bending, usually 0.3–0.4 eV, and a slightly larger measured decrease in work function followed by a gradual upward band bending and increase in work function with increasing coverage (Figure 6a). These changes level off near the 1-ML cutoff, and the work function eventually attains the value of a copper metal surface at higher coverage (4.8 eV for our unoriented Cu sample). Downward band bending and a lower work function with the initial 0.1-ML Cu deposition are also observed on the (10$\bar{1}$0) surface, but the changes were ~0.2 eV less than those observed on (000$\bar{1}$). Further copper evaporation again results in upward band bending and an increased work function. Copper deposition on ZnO (0001) results in only upward band bending and increased work function with increasing coverage as shown in Figure 6b.

These results can be interpreted by examining the initial band bending and work function properties of the three clean ZnO surfaces, which are decidedly different. The work functions measured by the biased He I spectra of the sputtered/annealed surfaces were 4.6 eV on (000$\bar{1}$), 4.3 eV on (10$\bar{1}$0), and 3.9 eV on (0001). Although these work functions are less than values obtained on cleaved surfaces, the relative values are quite similar to those in the literature.[64] The source of the surface-dependent work functions is primarily the large differences in band bending on the clean surfaces as reflected in the measured binding energies of the ZnO energy levels of the (000$\bar{1}$) surface, which were always 0.6–0.7 eV lower relative to the spectrometer Fermi level than on the clean (0001) surface.

The downward band bending with initial Cu deposition on (000$\bar{1}$) and (10$\bar{1}$0) is indicative of charge donation from the surface to the bulk. The magnitudes of the band bending changes upon initial Cu deposition (the difference between the two surfaces is quite close to the difference in the measured clean Zn 3d binding energies) indicate that they can be explained by the copper eliminating the initial depletion layer on these surfaces. The number of sites causing the depletion layer can only be on the order of <1% of the total surface sites (less than 1×10^{13} electrons), giving an upper limit to the number of Cu atoms donating electrons of ~1% of a monolayer.[65,66] This charge transfer, therefore, will have little effect on the chemical nature of the copper overlayer atoms. The upward band bending and increasing work function observed on these two surfaces after the initial downward movement and on the (0001) surface at all coverages arises from the contact potential difference of the ZnO surfaces and copper metal. The larger work function of copper metal (4.6–4.9 eV depending on surface plane) necessitates an upward band bending for the Fermi and vacuum levels of the interface components to become aligned. The higher Cu work function should result in the transfer of electrons from the substrate to the overlayer to align the Fermi levels of the two components. This charge transfer, however, does not produce a measurable chemical shift of the Cu $2p_{3/2}$ level to binding energies lower than observed for copper metal. The contact potential difference between the two species creates a Schottky barrier of 0.5–0.6 eV for the copper/ZnO interface, as measured by the total change in band bending from the initial Cu deposition to a highly Cu covered surface.

(B) Copper Coordination Chemistry. (1) Heating in Ultrahigh Vacuum. Perturbations were performed on submonolayer (0.3 ML) coverages on all three ZnO surfaces. The changes observed were always greatest for copper supported on the (0001) surface, and hence we focus on (0001) with comparison to the results on the other ZnO surfaces. In Figure 7b, the effects of heating on the Cu $2p_{3/2}$ peak of the 0.3-ML Cu/(0001) surface are shown. The surface was heated to the indicated temperatures and cooled back to room temperature for data collection. Heating to 523 K for 30 min decreases the intensity of the Cu 2p level by 20% while heating to 673 K for 30 min causes a 45% loss in Cu signal intensity relative to the Zn $2p_{3/2}$ core level. In addition, the Cu $2p_{3/2}$ peak shifts to lower binding energy relative to the substrate peaks (0.2–0.3 eV after heating to 673 K), and the peak becomes narrower. By comparison, the Cu $2p_{3/2}$ intensity of 0.3-ML/(0001) decreases by only <5% after heating to 523 K and 30% after heating to 673 K, while on the (10$\bar{1}$0) surface the changes were 20% at 523–573 K and 40% at 673 K. XPS data collected at the elevated temperatures show similar Cu peak intensities, binding energies, and peak widths as observed when cooled to room temperature, indicating that no reversible changes are detected by these methods.

LEED shows no new diffraction spots on any of the 0.3-ML surfaces after heating, only a sharpening of the (1 × 1) substrate pattern. Significant changes were observed upon heating a high coverage, 8 Å/(000$\bar{1}$) surface to 523 K. This surface had an initial Zn $2p_{3/2}$ I_θ/I_0 ratio of 0.27 and a very faint Cu (111) and the ZnO (1 × 1) LEED patterns. After heating, the I_θ/I_0 ratio increased to 0.57 while both the substrate and overlayer LEED patterns sharpened considerably.

The effects of heating on the valence band PES spectra of 0.3-ML Cu/(0001) are even more dramatic as shown in Figure 7d.[67] Heating to only 473 K causes a 45% decrease in the Cu 3d intensity (relative to the ZnO features) in the 120-eV spectrum of Cu/(0001) and an obvious movement of the Cu 3d states to

(64) Moorman, H.; Kohl, D.; Heiland, G. *Surf. Sci.* **1979**, *80*, 261.

(65) Morrison, S. R. In *Treatise on Solid State Chemistry*; Hannay, N. B., Eds., Plenum Press: New York, 1976; Vol. 6B, Chapter 3.

(66) Gopel, W.; Lampe, U. *Phys. Rev. B* **1980**, *22*, 6447.

(67) The Cu 3d intensities were determined by peak area measurement obtained by subtracting the clean ZnO spectrum from the appropriate Cu/ZnO data.

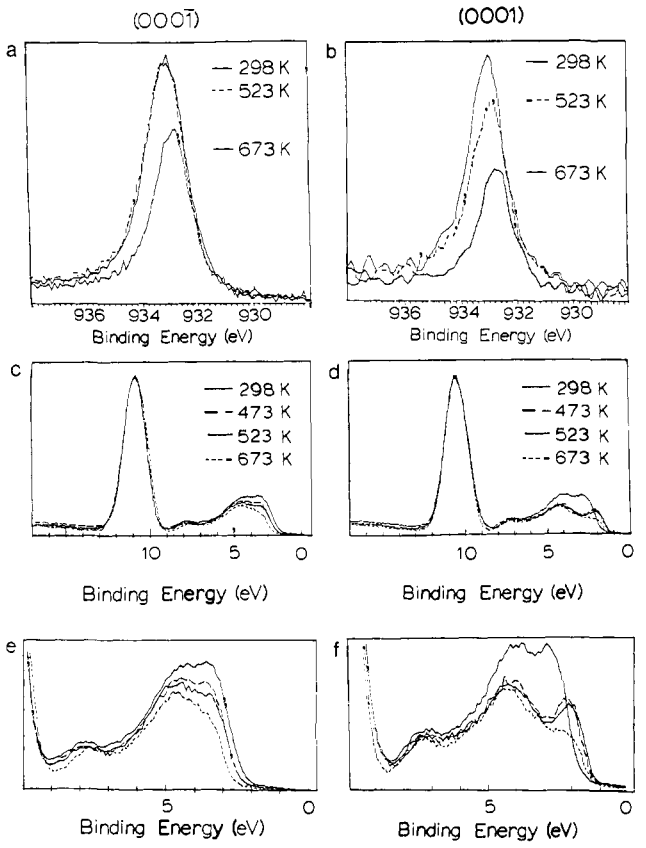

Figure 7. Effects of annealing 0.3-ML coverages to the indicated temperature on (a) the Cu $2p_{3/2}$ XPS peak on (000$\bar{1}$) and (b) (0001) and the 120-eV valence band spectra on (c) (000$\bar{1}$) and (d) (0001); (e) and (f) show (c) and (d) on an expanded scale (×2). Data were taken at room temperature.

lower binding energy, toward the Fermi level. Upon heating to 673 K, 60% of the Cu intensity is lost. By comparison, the valence band of 0.3-ML Cu on (000$\bar{1}$) does exhibit changes (Figure 7c), but again they are much less obvious than on (0001). The Cu 3d signal shows only a 20% decrease upon heating to 473 K and no significant shift to lower binding energy. Further heating to 673 K decreases the signal by similar amounts as on (0001), but no shift to lower binding energy relative to the substrate PES features is observed.

The loss of Cu overlayer PES intensity must be due to the loss of copper surface area which could result from several effects: loss of copper from the surface, diffusion of copper into the ZnO bulk, or the formation of three-dimensional copper particles. Several results indicate that surface diffusion followed by three-dimensional clustering is the dominant effect. First, extensive evaporation of copper from the surfaces at temperatures of 473–523 K is very unlikely as Chan and Griffen[41] report no significant Cu evaporation from a high-coverage Cu/ZnO surface below 750 K. Second, the binding energy shifts and shape changes of the copper core level are similar to those observed with increasing overlayer coverage, indicating the formation of a more bulklike, metallic copper on the surface. Third, the changes observed in the high Cu coverage surface LEED pattern with annealing imply the formation of larger, well-ordered Cu (111) surface area. Fourth, much larger intensity decreases in the more surface-sensitive valence band copper PES features as compared to the Cu $2p_{3/2}$ level are consistent with three-dimensional clustering. Finally, most of the copper core level intensity lost from the 0.3-ML Cu/(0001) surface because of the heat treatments can be restored by reaction with oxygen (vide infra), which indicates that the copper must remain on the surface of the ZnO crystal.

(2) Oxygen Exposures. The changes observed in the Cu $2p_{3/2}$ peaks after treating the 0.3 ML Cu/(0001) surface with molecular oxygen exposures are shown in Figure 8a. Room-temperature

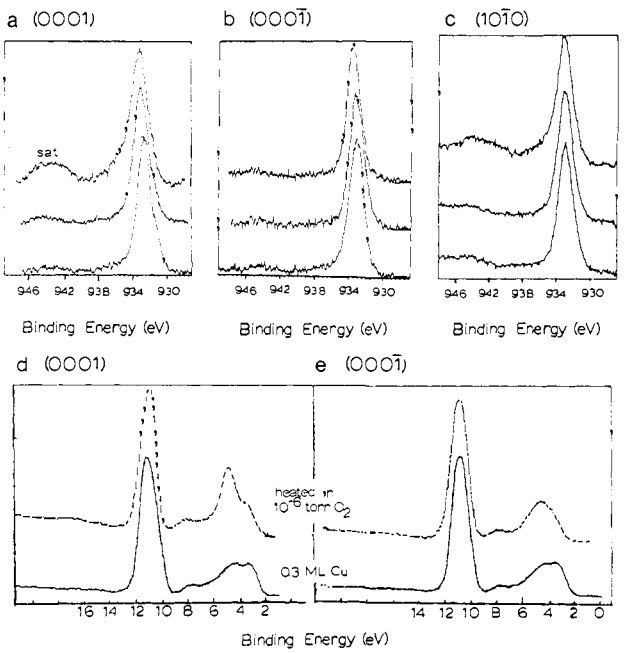

Figure 8. Cu $2p_{3/2}$ core level for 0.3-ML surfaces on (a) (0001), (b) (000$\bar{1}$), and (c) (10$\bar{1}$0) surfaces at room temperature (bottom), exposed to 100 langmuirs of O_2 at room temperature (middle), and heated to 523 K in 10^{-6} Torr of O_2 (top). The corresponding 120-eV valence band spectra for 0.3-ML surfaces before and after heating to 523 K in 10^{-6} Torr of O_2 are given in (d) (0001) and (e) (000$\bar{1}$).

exposures caused the Cu $2p_{3/2}$ level to shift to deeper binding energy by 0.25 eV relative to the ZnO features with exposures of 100 langmuirs (1 langmuir = 1×10^{-6} Torr·s) while the peak intensity remains the same. The valence band Cu states also shift to deeper binding energy. The core level changes of the 0.3-ML overlayers on the other surfaces are almost identical, as are band bending and work function changes, which saturate at ~100-langmuir exposure with the bands bending up by 0.2 eV and the work function increasing by ~0.5 eV.

At elevated temperatures, the oxygen treatments have a more substantial effect on the 0.3-ML Cu/(0001) surface as shown by the Cu $2p_{3/2}$ peak in Figure 8a. Following heating to 473 K in 1×10^{-6} Torr of O_2 (for 15 min = 900 langmuirs), the centroid of the Cu $2p_{3/2}$ peak for the Cu/(0001) surface shifts to deeper binding energy by ~0.6–0.9 eV relative to the 0.3-ML Cu surface, and a shoulder develops on the high binding energy side of the peak. The formation of shakeup satellite peaks at 8 eV deeper binding energy relative to the main Cu 2p peaks clearly indicates the formation of Cu^{2+} ions[68] on (0001), identifying the deeper binding energy shoulder on the main peak as resulting from Cu^{2+} photoemission, consistent with the chemical shift of Cu^{2+}. By comparison, the 0.3-ML Cu/(10$\bar{1}$0) surfaces also show the shift of the core level to deeper binding energy and the formation of smaller shakeup satellite peaks (Figure 8c). The amount of Cu^{2+} present on both (0001) and (10$\bar{1}$0) varied with surface treatment, although qualitatively, Cu oxidation was accomplished more easily on (0001). Although the Cu $2p_{3/2}$ peak shifts to deeper binding energy by ~0.6 eV, no shakeup intensity indicative of formation of cupric ions was observed for 0.3-ML Cu/(000$\bar{1}$) after any of the O_2 treatments in UHV (Figure 8b). For all surfaces, no significant copper 2p intensity is lost upon annealing in 10^{-6} Torr of O_2, even up to temperatures >573 K, although the main peak intensity does become redistributed into the satellite peak when Cu^{2+} is present, leaving the total intensity constant.

The cupric ions on the (0001) and (10$\bar{1}$0) surfaces are easily reduced by annealing to ~373–473 K in vacuum, with the Cu core level shifting 0.2 eV to lower binding energy and no loss of intensity. This behavior is consistent with the surface science literature concerning the oxidation of copper metal, where ex-

(68) Scrocco, M. *Chem. Phys. Lett.* **1979**, *63*, 52.

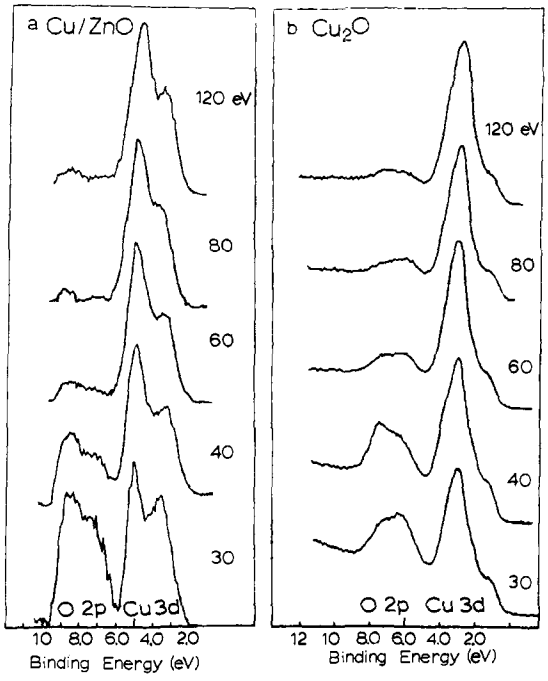

Figure 9. (a) Variable photon energy valence band difference spectra of 0.3-ML/(0001) heated in 10^{-6} Torr of O_2 compared to (b) the valence band spectra of Cu_2O. The spectra were obtained by subtracting the appropriate clean ZnO spectrum from the oxidized Cu/ZnO data.

tensive oxidation leads to cupric oxide and subsequent UHV anneals produce cuprous oxide.[62,69] Further annealing to 573–673 K in UHV decreases the Cu/Zn intensity ratio indicating a loss of copper surface area.

As mentioned above, oxygen treatments of a 0.3-ML Cu/(0001) surface that was previously heated in UHV provided an additional significant result. After annealing to 573 K in vacuum produced a 45% decrease in the XPS Cu/Zn core level intensity ratio, annealing to 523 K in 10^{-6} Torr of O_2 followed by a 473 K UHV anneal to eliminate the Cu^+ ions present regenerates ~90% of the lost copper $2p_{3/2}$ peak intensity. These results support the conclusions reached above concerning the formation of copper surface clusters upon heating in UHV and also show that an oxidizing agent plays two important roles in Cu/ZnO chemistry, keeping the copper in an oxidized form and dispersed on the ZnO surfaces.

Major changes in the shape of the valence band PES copper features at 3–5 eV binding energy for the dispersed copper on (0001) also occur with heating in oxygen ambients as shown in Figure 8d. The large changes are not observed upon heating clean ZnO surfaces in O_2 and can be associated with the copper overlayer. Difference spectra obtained by subtracting the clean ZnO spectrum from the data for 0.3-ML Cu/(0001) heated to 523 K in 10^{-6} Torr O_2 over a wide range of photon energies are shown in Figure 9a. The low photon energy difference spectra show two principle peaks, each of which is split, giving features at binding energies of 3.0, 4.5, 7.2, and 8.3 eV. The deeper binding energy features are most intense in the 30-eV data and decrease dramatically as the photon energy increases; comparison to theoretical cross sections[70] leads to their assignment as oxygen 2p photoemission not present in bulk ZnO. The lower binding energy feature with its relatively high intensity at higher photon energies results from ionization of the perturbed Cu 3d levels. The Cu d band is substantially altered by the O_2 treatments as compared to the d levels of the dispersed copper in Figure 4c. The two components of the d band have a different intensity dependence on photon energy. The lower binding energy component of the Cu 3d band gains in intensity relative to the deeper binding energy component as the photon energy is decreased, indicating significant admixture of oxygen 2p cross section in these copper levels. These results indicate the formation of a new copper oxide phase on the (0001) surface. Small changes are also observed on (000$\bar{1}$) in Figure 8e, but the extensive formation of this new copper site was not indicated.

Scheme II

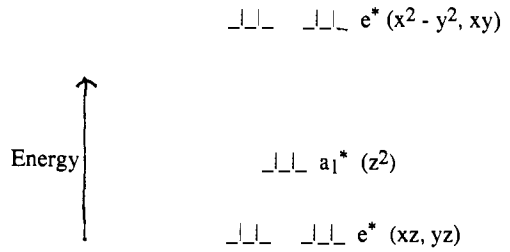

Comparison of the difference spectra in Figure 9a to the variable photon energy valence band spectra of Cu_2O provides insight into the nature of the copper oxide phase. The relative energy splitting of the copper and oxide features is almost identical for the two copper species. In addition, the relative intensities of the copper and oxygen peaks are quite similar for the two species at photon energies of 40 and 60 eV. The oxide peak of the oxidized Cu/ZnO spectrum at 30 eV is much larger than that observed for Cu_2O; however, there is a large uncertainty in the difference spectrum at this photon energy as the overlayer PES features are very weak compared to those of the ZnO substrate. The relative energy splittings of the Cu and O peaks and the qualitative intensity pattern strongly suggest that the oxidized copper phase is a Cu^+ oxide. An approximate quantitative comparison of the relative copper and oxygen peak intensities can be made to the theoretical atomic cross sections of ref 70. The data at 30 and 40 eV have Cu 3d:O 2p intensity ratios of 1.1–1.2:1 and 2.7:1, respectively, giving relative concentrations of 1.8–2.0:1 and 2.7:1, respectively. A 2:1 ratio is stoichiometrically correct for the oxidation of all copper present to Cu^+, and this is within the error of our calculation. Covalent mixing of the O 2p and Cu 3d levels would tend to increase the Cu 3d/O 2p intensity ratios at these photon energies as $\sigma_{2p} > \sigma_{3d}$, leading to a higher calculated Cu/O ratio than is actually present.

The shape of the Cu^+ oxide valence band spectrum should provide information concerning the bonding geometry of the Cu^+ surface site. The spectra in Figure 9a are significantly different from the valence band spectrum of Cu_2O shown at various photon energies[71] in Figure 9b. Cuprous oxide (where Cu has linear, 2-fold coordination) has a small PES peak at lowest binding energy resulting from the ionization of the most antibonding d_{z^2} orbital oriented along the linear bond axis. The oxidized Cu/ZnO d band has two peaks, with a photon energy dependent intensity ratio (1.74:1 at 120 eV, 1.45:1 at 80 eV, 1.35:1 at 40 eV, and ~1:1 at 30 eV) with the deeper binding energy peak being the more intense at high photon energy. These results indicate that the lower binding energy peak contains significantly more oxygen 2p character, and the overall intensity pattern and photon energy dependence of the d band show that the bonding in this phase is significantly different than that present in Cu_2O.

If epitaxial growth of this copper oxide phase occurs on ZnO, then a surface Cu^+ ion would be bound to three oxide ions, producing a coordinately unsaturated tetrahedral environment with a C_{3v} site symmetry. The Cu d-level splitting observed in the difference spectra of Figure 9a is consistent with the qualitative C_{3v} d-manifold energy level diagram given in Scheme II. The highest occupied $d_{x^2-y^2,xy}$ e set of orbitals is strongly σ-antibonding with the O 2p levels relative to the other d orbitals in this geometry. The a_1* level has both σ* and π* interactions, while the xz,yz e* energy level is only weakly π-antibonding. It should be noted that the actual splitting pattern will depend on the position of the

(69) Wertheim, G. K.; Hufner, S. *J. Electron Spectrosc. Relat. Phenom.* **1974**, *3*, 217.
(70) Yeh, J. J.; Lindau, I. *At. Data Nucl. Data Tables* **1985**, *32*, 1.
(71) Lin, J.; Didziulis, S. V.; Butcher, K.; Solomon, E. I., unpublished results.

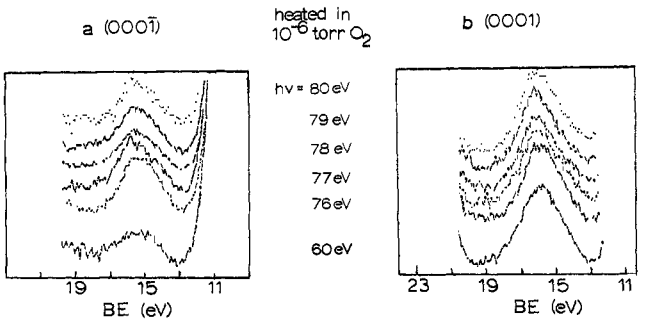

Figure 10. Resonance PES of the Cu satellite of oxidized Cu/ZnO surfaces obtained through the Cu 3p edge for (a) (000$\bar{1}$) and (b) (0001).

metal ion relative to the plane of oxide ions. The most important fact is that the x^2-y^2,xy e* energy level is the most strongly antibonding and will dominate the electronic structure. The PES spectrum of the C_{3v} Cu 3d band, therefore, should be split into two peaks having a 3:2 intensity ratio with the weaker, lower binding energy feature showing greater intensity modulation with photon energy due to the admixture of O 2p cross section as observed in our data.

Further evidence for a substantial change in the copper site upon oxidation is seen in the resonance PES data of the 0.3-ML Cu/(0001) surface in Figure 10b. The satellite off resonance intensity has increased dramatically and the resonance enhancement at the Cu 3p edge is substantially decreased. The $M_{2,3}M_{4,5}M_{4,5}$ Cu Auger peak that is so strong for copper metal and much weaker for the dispersed copper overlayer is absent in the oxidized Cu spectra at all photon energies. The large out-of-resonance satellite intensity is quite unusual for Cu^+ systems and indicates a large increase in the ability for charge to redistribute to compensate for the hole created by photoionization. Out-of-resonance satellite intensity requires a change in final-state wave functions that seems to be related to increased relaxation arising from greater 4s covalent mixing than either Cu_2O or CuCl. Similar changes are observed on the 0.3-ML Cu/(000$\bar{1}$) surface (Figure 10a); however, the extent of the changes is not as great. The possibility of Cu^{2+} ions causing the large out-of-resonance intensity must be rejected as the satellite peak is split too far from the main d band (12.5 eV) for an intense Cu^{2+} satellite (~9 eV) and some increase in the out-of-resonance intensity is observed on the oxygen treated Cu/(000$\bar{1}$) surface, where no cupric ions were observed with XPS.

(C) CO Chemisorption. The He II valence band spectrum of ZnO (10$\bar{1}$0) taken at 110 K in a 1 × 10^{-6} Torr ambient of CO is compared to the clean ZnO spectrum (dotted) in Figure 11a. The CO ambient spectrum has developed at least one new feature at 14.5-eV binding energy. When the clean ZnO spectrum at 110 K is subtracted from the CO ambient spectrum, the three-peak difference spectrum in Figure 11b is obtained. The three peaks in the difference spectrum correlate well to the three valence orbitals of CO, showing that the CO is chemisorbed molecularly to the surface. It is important to note that the difference spectrum shows that no other significant changes are occurring in the shapes of the ZnO features, indicating that the occupied Zn 3d levels are not measurably participating in the CO bonding. These results agree well with our previous work; the $4\sigma-5\sigma$ splitting (5.1 eV) is smaller than observed in the gas-phase photoelectron spectrum (5.6 eV), indicating that bonding is occurring primarily through the σ-bonding interaction of the carbon lone pair (5σ) with the empty Zn 4s.[1] Similar experiments conducted on the (0001) and (000$\bar{1}$) surfaces show a small 4σ peak on (0001) due to CO orientation effects and a very small 4σ peak on (000$\bar{1}$) due to the fact that CO chemisorbs only to step sites on the oxide surface shown in Figure 1.

When copper is evaporated onto the ZnO surfaces, their CO chemisorption properties are altered significantly. This is clearly observed in Figure 12a, where the He II spectra of (10$\bar{1}$0) are shown with increasing copper coverages from 0.1 to 1.0 ML at 130 K in a 1 × 10^{-6} Torr CO ambient. A small but observable

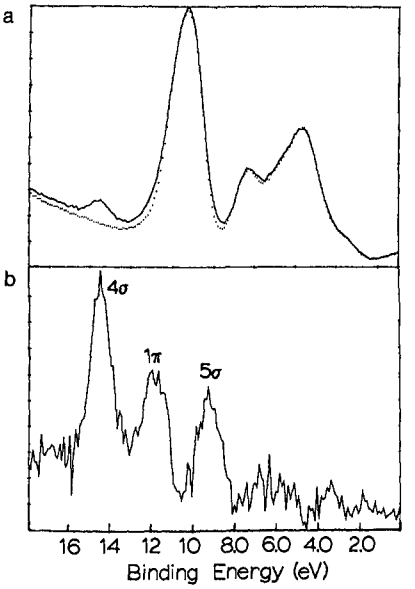

Figure 11. (a) He II valence band spectra of ZnO (10$\bar{1}$0) at 110 K in UHV (···) and in 10^{-6}-Torr CO ambient (—). (b) Difference spectrum obtained by subtracting the clean ZnO data from the CO chemisorbed data.

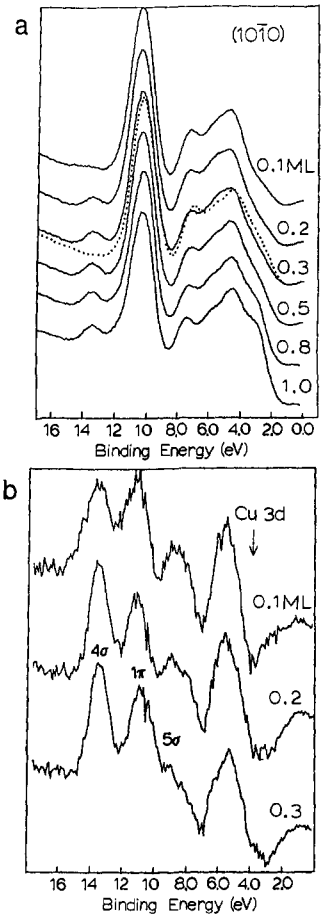

Figure 12. (a) He II spectra of Cu/ZnO (10$\bar{1}$0) taken at 130 K in a 10^{-6}-Torr CO ambient with increasing Cu coverage. From the top, the coverages are 0.1, 0.2, 0.3, 0.5, 0.8, and 1.0 ML. Also included are the 0.3-ML data taken prior to CO adsorption (···). (b) Difference spectra for the 0.1, 0.2, and 0.3 ML.

amount of CO chemisorbed to pure ZnO in our system under these conditions. The CO ambient spectra show the development of a new, broad, very weak peak near 14-eV binding energy for the 0.1-ML Cu surface. As the Cu coverage is increased to 0.2 ML, the peak increases in intensity and shifts to 13.6 eV. The peak

intensity further increases in the 0.3-ML spectrum, with the intensity changes closely following the increase in the amount of copper present on the surface. In addition, the CO is reversibly adsorbed to the copper sites at the temperatures studied as the 4σ peak decreases gradually with time if the CO ambient is pumped out. The original Cu/ZnO spectra are regained upon warming to temperatures near 200 K in the CO ambient. The difference spectra obtained by the subtraction of the appropriate 0.1-, 0.2-, and 0.3-ML Cu-covered spectrum from that obtained in the CO ambient show distinct three-peak spectra in the 8–14-eV binding energy region, characteristic of molecularly chemisorbed CO. These difference spectra in Figure 12b were obtained by normalizing both the intensity and binding energy scales of Cu/ZnO spectra with and without CO but are quite sensitive to the position of the background spectrum, making their interpretation somewhat tentative. Analogous to the CO–ZnO surface complex, the three peaks are assigned to the CO 4σ level at 13.5 eV, the 1π orbital at 11.0 eV, and the 5σ level at 8.5 eV, with the 4σ–5σ splitting of 5.0 eV approximately 0.6 eV smaller than the gas-phase spectrum and only slightly smaller than observed on ZnO. The broad 4σ peak in the 0.1-ML spectrum is attributed to CO chemisorption on both Zn^{2+} and copper sites. The 1-eV lower binding energy for the 4σ peak of the Cu–CO complex as compared to the Zn–CO derives from differences in final-state screening sometimes called extramolecular relaxation–polarization shifts.[72] The 13.5-eV binding energy of the 4σ peak, therefore, is used diagnostically to distinguish CO bound to surface copper species.

The 0.3-ML Cu/ZnO spectrum prior to exposure to CO is also included in Figure 12a to demonstrate the fact that important changes are occurring in the low binding energy region at energies corresponding to the 3d band of the copper overlayer atoms. These changes were observed in every Cu/ZnO–CO spectrum, were reversible as CO desorbed from the surface, and are more clearly observed in the difference spectra presented in Figure 12b. The difference spectra show that the chemisorption of CO is perturbing the copper electronic structure, with the chemisorption causing a portion of the d band to be shifted to deeper binding energy as evidenced by the loss in intensity in the 3–4-eV binding energy region and increase in the 5–6-eV region. These changes indicate that carbon monoxide is definitely bonding to the surface Cu atoms and that the Cu d levels are being stabilized by a bonding interaction with a higher energy CO level, most likely the $2\pi^*$ level. The results for 0.3 ML on (0001) at 130 K and 1×10^{-6} Torr of CO are quite similar to those obtained for the $(10\bar{1}0)$ surface at a comparable overlayer coverage. No such changes were ever observed for CO chemisorption to pure ZnO (see Figure 11).

A significantly different situation is observed for the 0.3-ML Cu overlayer on $(000\bar{1})$, where a CO 4σ peak is *not* observed under the conditions studied, ~130 K and at ambient pressures up to 5×10^{-6} Torr. No changes indicating CO chemisorption are observed in the valence band spectrum in the CO ambient, including the Cu 3d region, which was greatly perturbed on the other surfaces with CO chemisorption.

Adsorption isobars were obtained for CO chemisorption on the 0.3-ML Cu overlayers on both (0001) and $(10\bar{1}0)$ by varying the sample temperature in a constant-pressure CO ambient. The amount of CO chemisorbed was monitored by the intensity of the 4σ peak relative to the ZnO features as a function of both temperature and pressure. He II data were collected at a particular temperature until no change was observed for a given temperature, ensuring that the system had achieved equilibrium. With data obtained at different pressures, the isosteric heat of adsorption can be obtained from the Clausius–Clayperon equation:

$$(\mathrm{d} \ln p/\mathrm{d}(1/T))_\theta = -\Delta H_{ads}/R \qquad (4)$$

The isosteric heat of adsorption for a particular CO coverage θ for the two surfaces decreases with increasing CO coverage, a phenomenon observed for clean ZnO[1] and attributed to the repulsive interactions of the chemisorbed molecules. The heat of adsorption near zero CO coverage was estimated from the temperatures at which the smallest observable 4σ peak is present at pressures of 1×10^{-6} and 1×10^{-8} Torr. Consistent with the spectral similarities, the heats of adsorption for the two surfaces are determined to be 15 ± 2 kcal/mol on 0.3-ML Cu/(0001) and 16 ± 2 kcal/mol for 0.3-ML Cu/$(10\bar{1}0)$. These heats are significantly larger than observed on clean ZnO[1] (12 kcal/mol), consistent with our ability to discern CO chemisorption on copper sites from adsorption on the ZnO substrate. The ΔH_{ads} are in the range of the literature values for CO chemisorption on copper metal, which range from 10 to 16 kcal/mol.[34-37,73-76] Alternatively, the CO chemisorption results on the $(000\bar{1})$ surface place an upper limit of 12 kcal/mol for copper supported on this surface.

When CO chemisorption is studied on higher copper coverage ZnO surfaces (both the $(10\bar{1}0)$ and the $(000\bar{1})$ surfaces), the resulting He II spectra closely resemble those for CO chemisorption on copper metal. The spectra in Figure 12a obtained in the CO ambients show very little change in the 4σ peak intensity beyond 0.3–0.5-ML Cu overlayer coverage on $(10\bar{1}0)$. Other spectral changes occur in the 0.8- and 1.0-ML Cu spectra as evidenced by the increase in intensity between the 4σ and the Zn 3d peaks, resulting in a general loss of resolution of the CO features, with only the 4σ peak clearly distinguishable. The Cu d band continues to show changes indicative of backbonding interactions at these high coverages under CO chemisorption conditions. Upon increasing Cu coverage to 1.0 ML and higher on ZnO $(000\bar{1})$, a surface that will chemisorb a small amount of CO at 125 K under 1×10^{-6} Torr of CO is obtained. A three-peak difference spectrum is obtained where the two deeper binding energy features have approximately equal intensities and are separated by less than 2 eV, quite similar to the He II spectrum obtained by exposing copper metal single crystals to CO ambients at low temperatures.[77,78]

The changes in CO chemisorption induced by annealing the 0.3-ML Cu/(0001) and $(10\bar{1}0)$ surfaces in UHV were also examined. As discussed earlier, we have determined that annealing to 473–673 K causes primarily two-dimensional diffusion of copper on the ZnO surface followed by the formation of three-dimensional copper metal clusters. The 4σ intensities in the CO ambient spectra of annealed 0.3-ML Cu/ZnO surfaces decreased by >50% on the (0001) surface and ~45% on the $(10\bar{1}0)$ surface. A smaller intensity decrease is expected for the Cu core levels if three-dimensional copper clusters are being formed as the core level intensities will reflect some "bulk" Cu contributions while CO can only adsorb on surface sites. On both surfaces, the He II spectra are similar to those observed for CO adsorption upon increasing copper coverage and likely reflect the changes observed in the valence band spectrum from CO bonding to isolated Cu species to chemisorption on a more "metallic" Cu surface.

Finally, the CO chemisorption of 0.3-ML Cu overlayers on all three surfaces following 523 K anneals in a 10^{-6}-Torr ambient of O_2 was also studied with He II UPS. The 0.3-ML Cu/$(000\bar{1})$ surface, which did not adsorb CO at all before oxidation, shows little change after the O_2 anneal. The most striking change in CO chemisorption upon oxidation is observed on the (0001) surface, which is also the surface most prone to extensive copper oxidation. Figure 13 compares the room-temperature 0.3-ML Cu $2p_{3/2}$ main and shakeup satellite peaks with the low-temperature (130 K) valence band spectrum in 1×10^{-6} Torr CO ambient after various treatments. The spectra in part a are simply those obtained from the 0.3-ML Cu overlayer as discussed previously. After annealing to 523 K in 10^{-6} Torr of O_2 and cooling to <373 K in the O_2 atmosphere, the copper phase has been greatly perturbed, with the large Cu 2p shakeup peak in Figure 13b indicating that ~55% of the total copper present is Cu^{2+}.[79] The

(72) Rubloff, G. W.; Grobman, W. D.; Luth, H. *Phys. Rev. B* **1976**, *14*, 1450.

(73) Horn, K.; Hussain, M.; Pritchard, J. *Surf. Sci.* **1977**, *63*, 244.
(74) Kessler, J.; Thieme, F. *Surf. Sci.* **1977**, *67*, 405.
(75) Hollins, P.; Pritchard, J. *Surf. Sci.* **1979**, *89*, 486.
(76) Papp, H.; Pritchard, J. *Surf. Sci.* **1975**, *53*, 371.
(77) Jugnet, Y.; Duc, T. M. *Chem. Phys. Lett.* **1978**, *58*, 243.
(78) Demuth, J. E.; Eastman, D. E. *Solid State Commun.* **1976**, *18*, 1497.

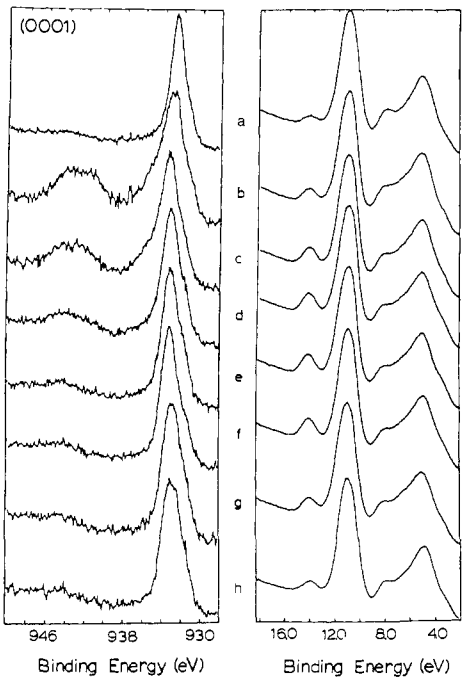

Figure 13. Cu $2p_{3/2}$ level (left) and the He II valence band spectra (right) at 130 K in 10^{-6} Torr of CO for 0.3-ML Cu/(0001). Spectra were obtained (a) as deposited, (b) after annealing to 523 K in O_2, (c) after 3 h at room temperature in UHV, (d) after annealing to 373 K, (e) after a second anneal to 373 K, (f) after 473 K anneal, (g) after 573 K anneal, and (h) after 673 K anneal.

valence band 10^{-6}-Torr CO ambient spectrum of the oxidized Cu shows a 1.6-fold increase in the CO 4σ peak intensity relative to the 0.3-ML surface prior to oxidation. After remaining at room temperature for several hours, the Cu 2p shakeup satellite intensity has decreased by 30% and the CO 4σ peak has increased by an additional 60% as shown in Figure 13c. Further sample anneals to 373 K (Figure 13d,e) and 473 K (Figure 13f) eliminate the Cu^{2+} shakeup peak, while the intensity of the main line approaches its value prior to oxidation, indicating the reduction of cupric ion sites. The CO 4σ peak intensity is maximized after the 473 K anneal, showing an increase by a factor of 1.9 relative to the spectrum taken immediately after oxidation. A strong correlation of the 4σ intensity to the number of Cu^{2+} sites reduced is indicated as the reduction of all Cu^{2+} sites (which comprised slightly more than half of the total surface sites) to CO chemisorption sites should produce an approximate 2-fold increase in CO 4σ intensity. Further anneals to 573–673 K decreased the intensity of the Cu core level, shifted it to lower binding energy indicating the formation of Cu metal clusters and gave smaller 4σ intensities as shown in Figure 13g,h.

The 4σ intensity on the Cu^+ sites on (0001) compared to the surface before oxidation is increased by a factor of 3 at 1×10^{-6} Torr, while at 1×10^{-7} Torr the intensity has increased by a factor of 4 and at 1×10^{-8} Torr of CO, the peak has increased by a factor of 5. This indicates that saturation coverage is being approached in the higher pressure regimes. Note that if the intensity increases after oxidation were solely due to a change in CO bonding geometry (which is possible because of the significant anisotropy of photoemission from the CO 4σ orbital[80]), then the 4σ increase should be a constant at the different pressures studied.

Greater amounts of chemisorbed CO on the Cu/(0001) surfaces after oxidation to Cu^+ should be reflected in a higher heat of adsorption assuming the number of available sites is the same. To determine the heat of adsorption of CO on the oxidized Cu phase, He II spectra were obtained over a wide range of temperatures in two different CO ambient pressures (1×10^{-6} and 1×10^{-8} Torr). These data are shown in Figure 14, where the change in 4σ intensity relative to the ZnO features is displayed as a function of measured sample temperature. The 4σ intensity was again taken as a measure of the amount of CO chemisorbed on the surface, and eq 4 used to determine ΔH_{ads}. The isosteric heat of adsorption was observed to decrease with increasing CO coverage. The value obtained from two experiments on surfaces prepared at different times gave a value of 21 ± 2 kcal/mol at zero coverage. The heat of adsorption, therefore, is substantially higher for the oxidized Cu^+ sites, a behavior we have now also observed on other Cu^+ sites in separate studies on single-crystal surfaces of CuCl and Cu_2O.[71]

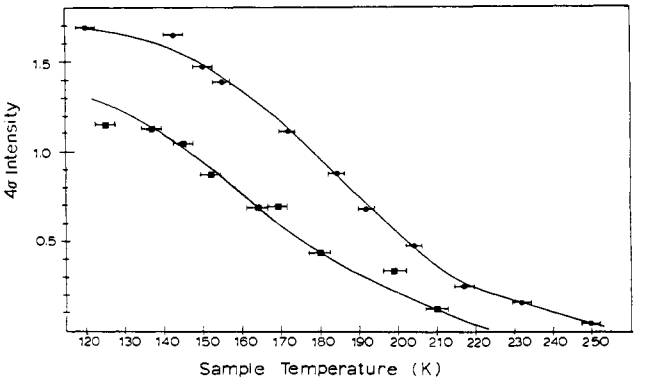

Figure 14. Plot of CO 4σ intensity on the oxidized Cu/(0001) surface as a function of temperature in 10^{-6}- (●) and 10^{-8}- (■) Torr CO ambients.

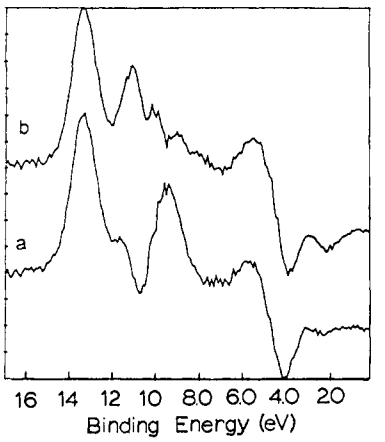

Figure 15. Valence band difference spectra of the 130 K, 10^{-6}-Torr CO ambient data of the oxidized 0.3-ML Cu/(0001) surface. The effect of shifting the clean spectrum in (a) by 100 meV is shown in (b).

The difference spectrum obtained by subtracting the (0001) oxidized/annealed 130 K spectrum before exposing to CO from the 130 K, 10^{-6}-Torr CO spectrum is given in Figure 15. The difference spectrum is extremely sensitive to the positioning of the background spectrum. With no energy shift of the background spectrum, a two-peak difference spectrum is obtained, with the peaks separated by ~4 eV (Figure 15b). If the background is shifted by 0.1 eV, then a two-to-three-peak spectrum is obtained, with the two deepest peaks separated by ~2.4 eV, with a possible third peak ~1 eV to lower binding energy from the second feature (Figure 15a). The large changes in the difference spectra incurred by such a small shift in the background limits the quantitative evaluation of the CO difference spectrum. We tentatively assign the relative CO peak splittings as 2.4 eV for the 4σ–1π and 4.0 eV for the 4σ–5σ. In addition, changes at low binding energy that are relatively insensitive to the positioning of the background spectrum are observed, with a loss of intensity at 3–4 eV and a corresponding gain in intensity at 5–6 eV. The low binding energy differences are comparable to those observed on the 0.3-ML surfaces prior to oxidation and indicate the participation of the Cu 3d levels in bonding with the CO molecule. These shifts appear

(79) The shakeup satellite is assumed to have 55% of the Cu(II) main peak intensity as observed in the CuO spectrum: Robert, T. *Chem. Phys.* **1975**, *8*, 123.

(80) Davenport, J. W. *Phys. Rev. Lett.* **1978**, *17*, 4908.

approximately equivalent for Cu^0 and Cu^+ surface sites, indicating similarities in the extent of π-backbonding for the two Cu sites.

Discussion

This section focuses on the portions of this work most relevant to the unique nature of the Cu/ZnO system and their possible effects on catalytic reactivity. We first discuss the electronic structure of highly dispersed copper supported on the single-crystal ZnO surfaces. The differing reactivity of copper supported on chemically different ZnO surfaces is then reviewed and discussed in terms of the Cu–ZnO surface bond. The production of several of the proposed copper active sites through selective perturbations and the interaction of these sites with carbon monoxide are then summarized. Finally, the implications of these results for understanding Cu/ZnO catalysis are explored, with an emphasis on the different possibilities for CO activation by copper sites versus Zn^{2+} sites.

The electronic structure of highly dispersed copper on the ZnO (000$\bar{1}$) and (0001) surfaces is significantly different from that of either Cu metal or Cu atoms. The differences are evident principally in the resonant PES results of the 0.3ML/ZnO surfaces (Table I), which show larger satellite 3d band splitting ($\sim$12.5 eV) than observed in Cu metal (11.7 eV), indicative of a greater electron Coulomb repulsion (U) for the dispersed Cu as compared to the metal. This result indicates that the orbitals of the dispersed copper atoms are more localized, which could lead to a greater tendency to participate in backbonding interactions. In addition, the resonant energies and presence of observable 4s photoemission intensity indicate that the copper is not oxidized by either of these surfaces. These results show that the dispersed copper has a somewhat different electronic structure that could effect the reactivity of this phase.

An important result of this work is the differing reactivity of the highly dispersed copper on chemically different ZnO surfaces. Although laminar overlayer growth on all three surfaces at room temperature and low Cu evaporation rates (1–2 Å/min) is implied by the XPS and LEED results, copper on the (000$\bar{1}$) surface is affected much less by heating in vacuum and oxygen atmospheres, indicating a stronger Cu–ZnO bond has occurred on the oxide-terminated surface. Three-dimensional copper clustering on heating in UHV and oxidation to some percentage of Cu^{2+} ions on heating in O_2 were both achieved most easily on the 0.3-ML Cu/(0001) surface while the 0.3-ML/(10$\bar{1}$0) exhibited some reactivity. The oxidation reactivity at high temperatures and the surface mobility of copper could be related as the Cu/(0001) surface displays the greatest tendency to form copper clusters on heating and is also the easiest to oxidize.

A bonding interaction between a copper atom and oxide ions on the (000$\bar{1}$) surface would result from the overlap of the metal atom's filled 3d, half-filled 4s, and empty 4p levels with the filled oxide 2p levels, unless the copper atoms prefer lattice defect sites at 0.3-ML. In the bonding interaction with oxides, the oxide ions would act as donor ligands and increase the electron density on the copper atom. This interaction is consistent with the CO chemisorption properties (vide infra) but is not implicated by any of the spectroscopic probes used in this study. Alternatively, Cu atoms on the (0001) surface must form bonds with the Zn^{2+} ions, and the high mobility and reactivity of these Cu atoms indicate that the Cu–Zn^{2+} acceptor interaction is weak.

These copper evaporation and selective perturbation experiments were instrumental in the preparation of a number of model active sites with different electronic structures on the chemically different ZnO surfaces. Highly dispersed copper sites at 0.3-ML coverage were chosen for further study as they represented the best compromise of atomic dispersion and reasonable signal/noise in the PES data. Larger copper clusters were available through two mechanisms, the evaporation of more copper onto the surfaces or through annealing the low-coverage surfaces in UHV, causing three-dimensional clustering. Finally, oxidized copper sites [Cu^+ and Cu^{2+}] were prepared through O_2 exposures of 0.3-ML overlayer surfaces. In particular, an unsaturated tetrahedral Cu^+ site was formed on the ZnO (0001) surface by annealing the sample to $\sim$523 K in a 10^{-6}-Torr O_2 ambient and then in a vacuum.

The CO chemisorption behavior of these model sites have definitively determined the site of high-affinity CO binding. The $\sim$15 kcal/mol heat of adsorption at zero coverage for the 0.3-ML Cu/(0001) and (10$\bar{1}$0) surfaces is quite similar to previous results on copper metal surfaces, although the He II difference spectra are somewhat different, displaying three well-defined peaks while the CO chemisorbed on Cu metal has strongly overlapping features in the 4σ–1π region. CO bonding to a Cu^0 site should result from the σ-donor interaction of the carbon lone-pair 5σ orbital with the Cu 4s and 4p and the π-acceptor interaction of the CO $2\pi^*$ level with the filled Cu d_{xz},d_{yz} levels. We see direct evidence of both of these interactions in the σ-stabilization of the 5σ CO level and the π-stabilization of the copper levels in the valence band PES data of the 0.3-ML Cu/(0001) and (10$\bar{1}$0) surfaces.

The dispersed 0.3-ML Cu/(000$\bar{1}$) surface did not chemisorb CO under 10^{-6}-Torr ambients at 130 K, indicating either a very low heat of adsorption (<12 kcal/mol) or an inaccessible adsorption site. A low heat of adsorption for copper supported on (000$\bar{1}$) could be explained by electron donation from the surface oxide ions, which appear to form strong bonds with the supported copper atoms as discussed above. Increased Cu 4s antibonding electron density would severly weaken the σ-bond formed by the 4s stabilization of the CO 5σ level. The predominant bonding interaction would then become the π-bond formed by the empty CO $2\pi^*$ level with the copper 3d levels, and apparently this is not strong enough to observe CO chemisorption under our conditions. A decreased ability for a metal to chemisorb CO has been observed on several other metal/metal oxide support systems and attributed to the "strong metal support interaction" (SMSI).[81] The source of SMSI is still being debated in the literature, with both electronic effects[82] (charge transfer of electrons from the substrate to the metal) and structural effects[83] (migration of the substrate on top of the metal atoms) implicated.

The strong CO chemisorption (21 kcal/mol) on the oxidized 0.3-ML Cu/(0001) surface defines the site of the high-affinity CO chemisorption as a copper(I) ion rather than Cu^0, Cu^{2+} or a modified Zn^{2+} site. In this work, the Cu^+ site apparently has a C_{3v} (unsaturated tetrahedral) geometry, although other studies conducted in our laboratory[71] indicate a similar heat of adsorption for CO on Cu_2O, where the copper has a linear, two-coordinate geometry. Neither the heat of adsorption nor the diffuse reflectance feature used by Klier, however, can distinguish CO chemisorption on a C_{3v} Cu^+ site or on a Cu_2O type site. The interaction of CO with a Cu^+ site should result in a much stronger σ-bond as the 4s level is now completely empty, producing a full σ-bond. This stronger σ-donation in combination with the π-acceptor interaction should create a stronger, shorter bond and therefore a much greater overlap of the CO 5σ and Cu^+ 4s level than is observed in either Cu^0 or ZnO, leading to greater stabilization of the 5σ level. This effect would explain the greatly perturbed CO difference spectra of Figure 15, with an apparent 4σ–5σ splitting of 4 eV (compared with $\sim$5 eV for both ZnO and Cu^0). The 21 kcal/mol value for the heat of adsorption is quite similar to the 22 kcal/mol calculated by Baetzold for a Cu^+ incorporated into the ZnO (10$\bar{1}$0) surface. Alternatively, Baetzold[84] calculated a very small ΔH_{ads} = 10 kcal/mol for a Cu^+ site in the (0001) plane, which is clearly inconsistent with our results. These results contradict the theoretical calculations of Rodriquez and Campbell, which predicted Cu^{2+} ions to be the most stable when substituted into the ZnO lattice and that the chemisorption of CO on these Cu sites would be similar to ZnO.[19]

These results have a number of significant implications with respect to Cu/ZnO catalysis. First, it appears that highly dispersed Cu is unstable on two of the predominant ZnO crystal faces

(81) Tauster, S. J.; Fung, S. C.; Garten, R. L. *J. Am. Chem. Soc.* **1978**, *100*, 170.
(82) Hicks, R. F.; Yen, Q.; Bell, A. T.; Fleisch, T. H. *Appl. Surf. Sci.* **1984**, *19*, 315.
(83) Sadeghi, H. R.; Henrich, V. E. *Appl. Surf. Sci.* **1984**, *19*, 330.
(84) Baetzold, R. C. *J. Phys. Chem.* **1985**, *89*, 4150.

exposed in Cu/ZnO catalysts, $(10\bar{1}0)$ and (0001). Reduced Cu atoms/small clusters on these surfaces tend to form larger three-dimensional metallic Cu clusters on heating to methanol synthesis reaction temperatures, which would diminish their catalytic effectiveness with time (an irreversible process in a reducing atmosphere). Alternatively, the presence of an oxidizing agent (O_2 in our experiments) maintains the copper dispersion and can reverse the clustering effects of reduction by forming more stable copper ions in oxide moieties on the surface. There is experimental evidence supporting the proposition that CO_2 in catalytic feed gas mixtures maintains Cu dispersion and oxidation state on catalyst powders[18,23] much as O_2 has done in this work. Heating the Cu/ZnO surfaces to 573–673 K in UHV tends to decrease Cu surface area whether reduced or previously oxidized, and methanol synthesis at these temperatures on Cu/ZnO has been observed to decrease much more rapidly with time. The single-crystal results are consistent with a "sintering" mechanism for loss of catalytic activity through the irreversible loss of copper surface area and associated decreased ability to chemisorb CO.

The different reactivity and CO chemisorption behavior of copper sites on different ZnO surfaces point to the possibility of the copper active site in methanol synthesis being associated with a particular ZnO plane. Campbell et al.[39] studied the methanol synthesis reactivity of high-coverage copper on the $(000\bar{1})$ surface and found negligible activity under the conditions studied (pressures $\leq$ 1500 Torr). This result is not surprising in light of our findings that high-coverage copper on $(000\bar{1})$ chemisorbs CO in a fashion similar to that of Cu metal (and hence should have reactivity similar to that of copper metal) and highly dispersed forms of Cu on the (0001) surface do not strongly interact with CO, again precluding methanol synthesis. It appears that other surfaces have properties that suggest them to be better candidates for reactivity studies. In particular, the dispersed copper on the (0001) is readily incorporated into the ZnO lattice as a Cu^+ site with strong CO chemisorption abilities and is, therefore, a likely possibility for high activity.

A stronger surface–CO bond does not require a lower activation barrier for the reaction as has been measured for methanol synthesis on Cu/ZnO unless the rate-determining step directly involves this surface species. The Cu–CO active site must provide a lower energy pathway for the reaction than a similar Zn^{2+}–CO complex to bring about the lower activation barrier for methanol synthesis. Baetzold[84] has calculated that a methoxy intermediate (one proposed reaction intermediate) is more stable by ~40 kcal/mol on a Cu^+ site, but the activation barriers for the conversion of CO to the intermediates are not known. Until a definite mechanism has been elucidated for this reaction, the nature of copper activation will remain the subject of much conjecture.

It is clear that there is a large change in the electronic structure of CO bound to Cu^+ compared to CO bound to Zn^{2+}. Two principal differences are the participation of the Cu 3d orbitals in a π-backbonding interaction with the CO $2\pi^*$ and also a stronger σ-donor interaction leading to a greater stabilization of the CO 5σ level. Both of these phenomena are evident in the difference spectra in Figure 15. Either effect could conceivably cause activation of the CO molecule; $2\pi^*$ occupation will weaken the C–O bond and perhaps make the molecule susceptible to proton attack. Increased 5σ donation would tend to polarize the molecule with a partial positive charge on the carbon atom and activate the molecule for hydride attack, which is the generally accepted mode of reactivity for CO hydrogenation in homogeneous sytems where formation of a formaldehyde intermediate from the carbonyl is the rate-determining step.[85] Further study of the Cu^+–CO interaction is essential to determine the electronic structure of the chemisorbed molecule, and our group is currently pursuing such studies on T_d Cu^+ sites on single-crystal CuCl surfaces. These studies should determine whether the donor or acceptor interaction dominates. It should be noted that the backbonding mode of activation does not rule out catalysis on dispersed Cu^0 since the π-bonding interactions occur on these sites as well. The Cu^+ sites would be more efficient sites for methanol synthesis, however, with their higher heats of CO chemisorption producing more surface-bound CO.

The issue of hydrogen activation has not been studied in detail for Cu/ZnO although the ability of ZnO to cleave H_2 heterolytically leads many to believe that the role of H_2 activation is limited to ZnO. It is interesting that Cu/ZnO (0001) is the surface on which the high-affinity CO site has been most readily prepared as this clean ZnO surface has also been shown to be highly active in alcohol deprotonation and decomposition reactions, implying its possible importance for the heterolytic hydrogen cleavage.[86,87] This suggests a possible source of the high catalytic activity of the Cu/ZnO system arising from the proximity of the CO chemisorption and hydrogen cleavage sites on the same ZnO (0001) surface.

Acknowledgment. We thank Jian-yi Lin for discussions of his work on the CO chemisorption on Cu_2O and CuCl. Acknowledgement is made to the donors of the Petroleum Research Fund, administered by the American Chemical Society, for support of this research. The Stanford Synchrotron Radiation Laboratory, which is supported by the U.S. Department of Energy, provided beam time for these experiments. The Stanford Center for Materials Research, which is funded by the NSF Division of Materials Research, provided experimental facilities.

Registry No. Cu, 7440-50-8; ZnO, 1314-13-2; CO, 630-08-0; O_2, 7782-44-7.

(85) Collman, J. P.; Hegedus, L. S.; Norton, J. R.; Finke, R. G. *Principles and Applications of Organotransition Metal Chemistry*; University Science Books: Mill Valley, CA, 1987.
(86) Cheng, W. H.; Akhter, S.; Kung, H. H. *J. Catal.* **1983**, *82*, 341.
(87) Bowker, M.; Houghton, H.; Waugh, K. C.; Giddings, T.; Green, M. *J. Catal.* **1983**, *84*, 252.